Antioxidant Properties of Breast Milk in a Caco-2BBE/HT29-MTX Cell Culture Model

By: Li Yao

A Thesis Submitted to the Faculty of Graduate Studies of

The University of Manitoba

In Partial Fulfillment of the Requirements of the Degree of

Master of Science

Department of Human Nutritional Sciences

University of Manitoba

Winnipeg

THE UNIVERSITY OF MANITOBA

FACULTY OF GRADUATE STUDIES

*****

COPYRIGHT PERMISSION

Antioxidant Properties of Breast Milk in a Caco-2BBE/HT29-MTX Cell Culture Model

BY

Li Yao

A Thesis/Practicum submitted to the Faculty of Graduate Studies of The University of Manitoba in partial fulfillment of the requirement of the degree

MASTER OF SCIENCE

Abstract

There is good evidence to suggest that human breast milk has antioxidant properties. Our primary goal is to investigate the effects of antioxidant properties of human milk on the neonatal gut.

An *in vitro* digestion model, which incorporates both gastric and intestinal phases, was developed. To model the human intestinal mucosa, Caco-2BBE cells and HT29-MTX cells were co-cultured on diluted Matrigel. After the addition of exogenous mucin, the co-culture was able to maintain its characteristics after 30-minute digested milk treatment.

Two relatively non- selective, oxidant-sensitive dyes revealed that both milk and digested milk alleviated oxidative stress in the co-culture. The comet assay, in contrast, indicated that *in vitro*-digested milk exhibited less efficacy in reducing oxidative DNA damaged than milk, likely due to the compromise of antioxidant compounds during the *in vitro* digestion process. Our results conformed that the notion that breast milk reduces oxidative stress in a physiological system.

Acknowledgements

In the beginning, I would like to acknowledge my committee members. First, I express my gratitude to supervisor, Dr. James K. Friel. I appreciate that he gave the opportunity to participate in this study. Without his financial support and confidence in me, I would not finish my study. Secondly, my thankfulness goes to Dr. William Diehl-Jones. It is his constant and patient instruction that inspired me to complete my thesis. His encouragement motivated me to overcome failure and setbacks. I also thank Dr. Miyoung Suh for her creative advice and original insights into my project.

My special thanks go to Dr. Thomas Kissel and Per Artursson for their kind donation of HT29-MTX cells. Also, I am grateful to my colleagues, Apollinaire Tsopmo, Sunjay Lakhi, Ryan Szajkowski, Divna Garlic and Soherla Najafi. Their technical assistance throughout study gave me the strength to complete this study. My gratitude goes to Trisha Pownall for proofreading this thesis. I thank nurses and mothers who engaged in this study. This project could not be accomplished without their participation.

Finally, I thank Manitoba Institute of Child Health and Advanced Foods & Materials Network for their financial aid.

Table of contents iii, v

Chapter 1 Rationale

Infants are considered to be premature if gestation is less than 37 weeks (1). Supplemental oxygen therapy is usually administered to premature infants due to their immature respiratory systems (2). The transition from hypoxic environment to hyperoxic environment may result in excessive production of reactive oxygen species (3). This overproduction of reactive oxygen species may overwhelm the immature antioxidant defense systems of premature infants, thereby inducing oxidative stress. As a result, premature infants often suffer from oxidative stress-related diseases, including necrotizing enterocolitis, chronic lung disease, bronchopulmonary dysplasia and retinopathy of prematurity (4-7).

Exclusive breastfeeding is recommended to infants less than six months of age because human milk has antimicrobial factors, antibodies, hormones and growth factors. In addition, accumulating evidence has shown that human milk has strong antioxidant properties (8, 9). Antioxidant compounds in breast milk may function to protect premature infants from oxidative stress-related diseases.

Chapter 2 Literature review

2.1 Oxidative stress

2.1.1 Reactive oxygen species

Reactive oxygen species (ROS) form as natural byproducts of the normal metabolism and are essential in many biological processes, including cell signalling (10). Examples of ROS include superoxide anion ($O_2^{\bullet -}$), hydroxyl ion (HO•), ozone, singlet oxygen and hydrogen peroxide (H_2O_2).

When ROS are generated in excessive amounts and overwhelm the body's cellular antioxidant defense systems, they have the potential to destabilize other molecules, including proteins, lipids and nucleic acids, by either acquiring or donating electrons, which renders these molecules unstable. The following equations depict how ROS are formed (7). A superoxide anion is formed when an oxygen molecule (O_2) acquires an additional electron (e-).

$O_2 + e^- \longrightarrow O_2^{\bullet -}$

Normally, superoxide anions are short-lived and are converted to hydrogen peroxide molecules by the enzyme superoxide dismutase.

$$2\, O_2^{\bullet -} + 2H^+ \xrightarrow{\text{superoxide dismutase}} H_2O_2 + O_2$$

Hydrogen peroxide molecules can react with superoxide anions, resulting in the formation of hydroxyl radical (11).

$O_2^{\bullet -} + H_2O_2 \longrightarrow O_2 + HO^- + HO^{\bullet}$

2.1.2 Antioxidant defense mechanisms

Antioxidants delay or inhibit oxidation. They play a central role in defending against ROS damage in all organisms (12). Generally, they are divided into two categoriess: enzymatic antioxidants and non-enzymatic antioxidants.

Enzymatic antioxidants, including superoxide dismutase (SOD), glutathione peroxidase (GPx) and catalase (CAT), protect our biological systems from ROS damage. SOD catalyzes the dismutation of superoxide into oxygen and hydrogen peroxide, providing antioxidant defense in nearly all cells exposed to oxygen (13). GPx is the general name of an enzyme family with peroxidase activity that protects the organism from oxidative damage. It accelerates intracellular reduction of hydrogen peroxide to water and glutathione disulfide from glutathione (7). CAT detoxifies hydrogen peroxide to water and oxygen.

Non-enzymatic antioxidants can be derived from nutrients, such as Vitamin A, Vitamin C, Vitamin E and beta-carotene. A number of minerals, including selenium, zinc, iron, copper, manganese, also have antioxidant properties.

Vitamin A is an essential human nutrient that exists in several forms. β-carotene is a vitamin A precursor carried in plasma and LDL-cholesterol (14). It reduces oxidized LDL uptake, but does not prevent LDL oxidation. Vitamin C, also known as ascorbic acid, is a water-soluble vitamin. It scavenges plasma free radicals and is the predominant plasma antioxidant. Furthermore, it regenerates active vitamin E and increases cholesterol excretion. Vitamin E is a fat-soluble vitamin, which also exists in several forms. The most active and available form of vitamin E is

α-tocopherol. It is incorporated into lipoproteins and cell membranes, limiting the perioxidation of polyunsaturated fatty acid in membranes.

Lactoferrin is an iron-binding glycoprotein, which belongs to the transferrin family. Lactoferrin is considered to be an antioxidant because it is able to bind two atoms of iron that participates in the production of free radicals (15). Lysozyme is a member of highly conserved host-defense proteins. It has been found that the 18-amino acid domain of lysozyme exhibits a high affinity for advanced glycation end products that contribute to the ROS formation (16).

Flavonoids are polyphenolic compounds that are ubiquitous in nature and can be classified into several groups, including flavonols, flavones, flavanones and isoflavones. Flavonoids can replace vitamin E as chain-breaking anti-oxidants and scavenge superoxide anions, singlet oxygen, and lipid peroxy radicals. In addition, flavonoids can sequester metal ions, which engage in free radical formation through ligand-binding and therefore inhibit oxidation of low-density lipoproteins (17).

2.1.3 Oxidative stress

Oxidative stress occurs when oxidants in the body overwhelm antioxidants, leading to potential cellular damage (12). Damage caused by oxidative stress accumulates progressively as people age. Ultimately, this may lead to cell death and dysfunction of organs and the central nervous system.

Many diseases, including adult disorders such as atherosclerosis, cancer, cardiovascular diseases, and neurodegenerative disorders, may be related to oxidative stress (18). In premature infants, the excessive production of ROS is also thought to be linked to bronchopulmonary dysplasia (BPD) or chronic lung disease (CLD), retinopathy of prematurity (ROP), Respiratory distress syndrome (RDS) and necrotizing enterocolitis (NEC) that are commonly found in premature infants (PT), especially if they are incubated in an atmosphere with very rich oxygen concentrations (higher than 70% oxygen saturation) (18).

2.2 Premature infant

2.2.1 Preterm infants and complications of prematurity

The normal gestational period for human full-term infants (FT) ranges from 38-42 weeks. Preterm infants (PT) are babies born before 37 weeks of completed gestation (5). The weight of PT at birth is usually less than 2,500 g, while very low birth weight premature infants weigh less than 1,500 g due to immaturity. A history of preterm birth, diabetes mellitus, hypertension, smoking and consumption of alcohol are factors leading to premature labour (19).

Due to improvements in neonatal intensive care, the incidence of preterm births in Canada has increased from 6.3 percent of live births in 1981 through 1983, to 6.8 percent in1992 through 1994, a relative increase of 9 percent (20). The survival rate of preterm infants is increasing because of medical advances in neonatal intensive care and management of high-risk pregnancy.

Due to the immature development of the premature infant body system, this vulnerable group in the population is at a higher risk of developing certain diseases (Table 1). Among these disorders, specific complications, such as ROP, NEC and RDS, have a significant impact on long-term development of PT (21).

NEC is defined as an acute inflammatory necrosis process of the intestine that is commonly seen in preterm infants (22).The etiology of NEC is still unknown and the key risk factors leading to NEC in premature infants are prematurity, enteral feeds, intestinal ischemia, mucosal injury and bacterial colonization. Approximately 5-10% of very low birth weight premature infants suffer from NEC and overall mortality rate for NEC is as high as 25% for premature infants (24). Treatments for NEC are switching regular feedings to intravenous (IV) catheters, antibiotic therapy surgery and human milk feeding (23, 24).

ROP is defined as a process of abnormal neovascularisation because of extreme prematurity, hyperoxia and retinal ischaemia (21). The incidence of ROP is inversely linked to gestational age and serious ROP leading to retinal detachment and blindness is more likely to occur in infants with birth weight less than 1000 g. To avoid hypoxia, supplemental oxygen is supplied to premature infants, which can cause the retinal vessels to constrict to the point of obliteration. In addition, oxygen induces the production of ROS that can override the antioxidant defense system of premature infants.

RDS is believed to be the leading cause of mortality and morbidity in preterm infants (25). The features of RDS include impaired gas exchange, decreased static

compliance and non-hydrostatic pulmonary edema due to the loss of the integrity of the alveolocapillary barrier with impairment of normal surfactant function. Respiratory distress syndrome can be caused by many factors, but a lack of surfactant is believed to be the determining factor (23).

2.2.2 Hypoxia/ hyperoxia and overproduction of ROS in premature infants

Three factors subject premature infants to hypoxia (deficiency in the amount of oxygen reaching body tissues) immediately after birth. First, premature infants face external environment with relative high concentrations of oxygen after birth in comparison with those of the womb (3).

Secondly, RDS occurs often in premature infants because of the surfactant deficiency at the gas-liquid interface. Their lungs have difficulty in exchanging sufficient oxygen for body organs (21). Thirdly, due to depressed cardiac output, vasoconstriction of critical vascular beds and low blood pressure, ischemia (a decrease in the blood supply to body organs) is commonly observed in premature infants, causing insufficient lung oxygen transported to body organs (26).

To treat hypoxia, supplemental oxygen therapy is routinely administered to postpartum premature infants and oxygen supply is increased from 21% (room air) to 70-90% and may reach 100% (2). This high inspired oxygen concentration (FiO_2) facilitates the exchange of oxygen and increases arterial oxygen supply to postnatal premature infants, but may also cause hyperoxia (excessive amount of oxygen reaching body tissues).

When exposed to hypoxia, the production of SOD in premature infants is down-regulated. In addition, hypoxia at birth leads to a breakdown of ATP to hypoxanthine and a conversion of xanthine dehydrogenase to xanthine oxidase (XOD), the main free radical-producing enzyme in our bodies (27). These changes undermine the immature antioxidant defenses of premature infants. When supplemented O_2 is supplied to premature infants, the diminished antioxidant defenses often are unable to counterbalance the increased load of oxygen free radicals.

2.2.3 Premature antioxidant enzymes in pre-term infants

Due to incomplete gestation, premature infants lack antioxidant enzymes to protect them from excessive production of ROS. The activities of antioxidant enzymes, such as SOD, CAT, GPx, in guinea pig lungs and livers were determined over the final period of gestation by Rickett et al (28). Marked increases in pulmonary antioxidant enzymes were found over the final period of gestation. For example, GPx activity in the fetal lungs almost doubled between day 50 gestation and birth. Pulmonary Cu/Zn-SOD activity continued to increase until post-partum.

Liver antioxidant capacity exhibited similar developmental pattern found in lungs. Liver Cu/Zn-SOD activity increased 10 times pre-partum. Liver Mn-SOD activity displayed a similar trend as Cu/Zn-SOD. A seven-fold increase in CAT activity was observed during pre-birth period. Liver GPx reached the peak prior to birth.

Dobashi et al. (29) studied CuZn-SOD and Mn-SOD in the lungs of human fetuses and newborn infants using immunohistochemical technique. Results indicated that staining for CuZn-SOD and Mn-SOD increased 30-fold and eight-fold from 16 to 38 weeks, respectively. Moreover, a marked decrease in CuZn-SOD staining was seen in lungs with respiratory diseases.

Experiments from animals and humans indicate there are dramatic increases in activities of antioxidant enzymes over the final period of gestation. Therefore premature infants born before complete gestation have a weak enzymatic antioxidant defense system.

2.2.4 Evidence of oxidation caused by ROS in premature infants

Most ROS *in vivo* are difficult to measure directly because of their high reactivity and relative instability. Thus, ROS are usually measured indirectly by measurement of their stable oxidative products.

A study conducted by Inder et al. (30) compared free radical products in the cerebrospinal fluid (CSF) of premature infants having cerebral white matter injury (WMI) with that of premature infants, full-term infants and adults without WMI. Lipid peroxidation products, 8-isoprostane, malondialdehyde (MDA), protein oxidation products and protein carbonyls were measured. Data indicated that premature infants with white matter injury had a significant elevation in CSF protein carbonyl levels (generally two-fold) compared to premature infants, term infants, and adult subjects without white matter injury. A trend toward an elevation of

8-isoprostane levels was found in the premature infants with white matter injury in comparison with those without white matter injury.

In a study conducted by Buonocore et al. (31), cord blood was drawn immediately after delivery and on day seven after birth from 34 hypoxic and 15 control preterm infants. Plasma levels of hypoxanthine (Hx), total hydroperoxide (TH), and advanced oxidation protein products (AOPP) were measured. Plasma Hx, TH, and AOPP levels were significantly higher in hypoxic infants than in control infants at birth and on day seven. There were statistically significant correlations between AOPP and Hx and between AOPP and TH levels on day seven. In addition, data indicated that the production of TH and AOPP was prolonged for several days after birth in hypoxic preterm infants.

2.2.5 Diseases of premature infants due to ROS

Common diseases, including NEC, BPD, CLD and ROP in premature infants are thought to be closely linked to inadequate protection against oxidative stress. The incidence of NEC is very high in premature infants and hydrogen peroxide molecules are thought to play a major role in it. Okur et al. (6) developed an experimental model to mimic the hypoxic / hyperoxic condition encountered by premature infants. Ten one-day-old Wistar albino rat pups were exposed to hypoxic conditions for 5 min (100% CO_2). At the end of this period, rat pups were cyanotic and gasping, but no death resulted. Animals were reoxygenated with 100% oxygen for 5 min and then all the subjects were kept in normoxic conditions for 2 days and then were sacrificed on day 4 after birth. A histological study was run on the distal

small bowel and localized hemorrhagic lesions similar to the findings seen in neonatal NEC were found. Additionally, intestinal tissues were homogenized and the MDA levels in homogenates were measured. The MDA levels were significantly higher in comparison with control group (1-day-old wistar albino rat pups living in normal condition). Okur et al. (6) concluded that hypoxia played an important role in the pathogenesis of NEC.

Ogihara et al. (7) measured the lipid oxidation products of premature infants in plasma in the first week of life. There were higher plasma concentrations of heptanal, 2-nonenal and 4 hydroxynonenal, in the first day of life in infants who developed BPD compared to those who did not. In another study, Nycyk et al. (7) found that infants who developed BPD had higher exhaled pentane, a type of lipid oxidation product, on the first day of life than patients who did not develop BPD. These results indicate that infants are under oxidative stress in their early life.

To test the relationship between ROP in premature infants and oxidative stress, Munguia et al. recruited 50 premature infants of less than 33 weeks gestational age and determined serum lipoperoxide levels to measure oxidative stress (4). The mean values of serum lipoperoxides showed a significant difference between infants who developed ROP (5.44 +/- 1.30 nmol/ml) and those who did not (2.94 +/- 0.89 nmol/ml, $p = 0.0001$). They concluded that there was a link between high serum lipoperoxide levels, as a measure of oxidative stress, and the incidence of ROP in premature infants.

In a study of the relationship between premature infants with CLD and ROS, plasma allantoin, the most abundant oxidation product of uric acid and a sensitive marker of oxidative stress, and allantoin/uric acid ratio were measured (5). Elevated plasma allantoin and allantoin/uric acid ratio were found in CLD group (neonates with clinical signs of respiratory distress, abnormal chest radiographs, and persistent oxygen requirement) compared with the control group (neonates without clinical or radiological signs of RDS and in need of oxygen supplementation).

As discussed previously, premature infants are at risk of excessive ROS, consequently suffering from diseases either caused by or associated with oxidative stress. An optimal supplemental oxygen supply to premature infants, to large degree, can decrease ROS damage. Although some recommendations of optimal supplemental oxygen supply for premature infants are available, they are probably more suitable for the more mature premature infants, not for growing extremely low birth weight premature infants (32). In addition to closely monitoring and managing oxygen therapies, an adjunct approach to prevent free radical-related diseases in neonates is to optimize feeding protocols for premature infants. Human breast milk, the optimal food for infants, has been shown to confer antioxidant effects (8). The relevant properties of milk will be reviewed in the following sections.

2.3 Human milk

2.3.1 Composition of human milk

Human milk predominantly consists of water, carbohydrates, fats, proteins, minerals and vitamins. The main nutrients in 100 ml breast human milk from mothers of mature infants are shown in Table 2.

Proteins in infant formulas are usually derived from cow's milk. Even though there are many similarities between human milk and cow's milk, some components differ significantly from each other. The ratio of casein to whey protein in human milk is 1:4; in cow milk it is 4:1 (1). In cow's milk, 20% of calories derive from protein, but in human milk, protein accounts for only 6% of total energy. The content of lactose and fat is higher in human milk than in cow's milk. Additionally, minerals, such as calcium, phosphorus, magnesium, are much higher in cow's milk (1).

2.3.2 Beneficial effects of human milk

Breast milk is regarded as the best food for preterm infants, since it benefits them from nutritional, gastrointestinal, immunological, developmental, and psychological perspectives (33). The patterns of amino acids and fatty acids in human milk provide unique advantages to preterm infants. Unlike bovine milk, which whey proteins and β-lactoglobulin may cause allergy and colic, whey proteins in human milk are easily digested. In addition to providing 50% calories in human milk, the pattern of fatty acids and presence of bile salt-stimulated lipase promote the absorption of fats.

Whey proteins in human milk promote gastric emptying. Furthermore, nutrients including amino acids, peptides and glycoproteins, and other components, such as hormones, epidermal growth factor, nerve growth factor facilitate gastrointestinal maturation.

Human milk plays an important role in the buildup of premature infant immune system. Lysozme, immunoglobulin A, lactoferrin and interferon in human milk protect infants from infection. It has been shown breast feeding significantly lowers NEC in infants in comparison with formula feeding (34). Many studies have reported that breast-feeding was associated with significantly higher scores for cognitive development than was formula feeding (9, 35). Moreover, human milk feeding fosters greater mother-infant attachment (33).

2.3.3 Antioxidant properties of human milk to defend against ROS

Human milk not only provides essential nutrients to meet premature infant growth, but it also contains some compounds, which may enhance infant immature antioxidant defense systems. Antioxidant enzymes, including GHSPx, SOD and CAT, and vitamin A, E in human milk are believed to assist in the destruction of H_2O_2 (9, 36). Scavengers of free radicals, including alpha-tocopherol, cysteine and ascorbic acid, are considerably higher in human in comparison with cow milk (37).

Shoji et al. (38)conducted research on whether breast milk can act as an antioxidant in infants. Spot urine samples were collected from forty-one healthy one-month-old infants (twenty-three males and eighteen females). Based on types of

feeding subjects were classified into four groups. The breast-fed group was defined as obtaining more than ninety percent of their caloric intake from breast milk. The breast milk dominant mixed-fed group was defined as obtaining fifty percent to ninety percent of their caloric intake from breast milk. The artificial milk dominant mixed-fed group was defined as obtaining fifty percent to ninety percent of their intake from formula. The formula-fed group was defined as obtaining more than ninety percent of their intake from formula. Urinary 8-hydroxy-2'-deoxyguanosine (8-OHdG), one of the biomarkers of oxidative DNA damage, was measured and data suggested urinary 8-OHdG excretion of the breast-fed group was significantly lower in comparison to those of the artificial milk dominant mixed-fed group or the formula-fed group. The researchers concluded that breast milk showed better antioxidant effects during infancy than artificial formula.

Research conducted by Friel et al. (8)showed that human milk provided better antioxidant protection than formulas. Physiological oxidative stress was induced to breast milk and infant formulas by hypoxanthine/xanthine oxidase and ascorbate free radical electron spin resonance (ESR) intensity, a marker for the degree of ongoing free radical oxidative stress, was monitored. Results from ESR analyses indicated that the initial background of free radical production was higher in formula than that in HM samples at all times. They also observed that oxygen consumption was always faster in formula compared to breast milk samples. Their result suggested that breast milk provides better antioxidant protection than infant formula

2.3.4 Breastfeeding

After birth, exclusive breastfeeding is recommended for the first 6 months of life (39). For infants, oral feeding is one of the most complicated developmental neuro-muscular tasks, including sucking, swallowing, and respiring (40). Preterm infants are known to have difficulty coordinating suck, swallow and respiration, therefore being inappropriate for oral feeding administration (41). Mothers of VLBW infants often have to pump their milk for gavage feeding until their infant is physiologically ready for normal breastfeeding (42). Despite the beneficial effects of human milk, expressed breast milk is not always available. As an alternative, a variety of artificial formulas, mainly modified cow's milk are used to feed preterm infants (43).

2.3.5 Advantage of human milk over infant formulas

Unlike bovine milk proteins that may cause allergy, human breast milk is easily digested and facilitate gastric empty (33). In addition, the presence of active enzymes in breast milk promotes the maturity of the underdeveloped gut, and anti-infective compounds protect the newborn from infection (44).

Shoji et al. (9)investigated the antioxidant protection of breast milk over IEC-6 cells, a non-transformed rat intestinal crypt cell. In the study, confluent IEC-6 cells were pre-incubated with 100-time diluted defatted human milk or three commercially available formulas. Oxidative stress was then induced by challenging cells with 0.5 mM of hydrogen peroxide for 30 minutes. Results demonstrated that

human breast milk treatment alleviated hydrogen peroxide-induced oxidative stress, whereas this antioxidant capacity was not shown in formulas treatment.

In a study conducted by Ayciek et al. (36), term infants were fed breast milk or a cow's milk modified formula. Biomarkers of oxidative status, including plasma total antioxidant capacity (TAC), total peroxide (TP), and oxidative stress index (OSI) were measured. Plasma TAC and vitamin C levels were significantly higher in the breast-fed group, while plasma TP levels and the OSI were higher in the formula-fed group. These researchers concluded that breast milk provides better antioxidant potential than do formulas.

As discussed above, in addition to intrinsic nutritional, gastrointestinal, immunological benefits, breast milk has its unique antioxidant properties, which are not found in infant formulas. Premature infants are at risk of oxidative stress, but the inabilities to be breastfed make human milk unavailable to them without specialized feeding tubes such as nasogastric or orogastric catheters. Unique infant formulas with antioxidant properties could be good alternatives to human milk to confer antioxidant protection for premature infants.

Chapter 3 Study design

3.1 Hypotheses

1) Digestion of human milk leads to different products of oxidation than are present in undigested milk alone.

2) Breast milk can decrease oxidative stress in a Caco-2BBE/HT29-MTX cell culture mimicking neonatal gut.

3.2 Objectives

The overall objective is to study the effects of *in vitro* digested breast milk on the oxidative state in an enterocytes model. To this end, three primary goals are proposed:

1. Develop an *in vitro* digestion system to mimic preterm infant digestion;

2. Develop a Caco-2BBE/HT29-MTX cell model mimicking the neonatal gut;

3. Test the effects of the *in vitro* digested breast milk on the oxidative state of the Caco-2BBE/HT29-MTX cell model.

3.3 Study design

3.3.1 Collection of milk samples

Milk samples (n=21) for this study were collected from twenty-one preterm infant mothers (born between twenty-nine and thirty-seven weeks of gestation) during the second week of lactation. Consent and ethical approval according to

University of Manitoba Human Research Ethics Board (HREB) was obtained from women who participated in the study. Milk samples were collected by the mother using a breast pump or by hand expression and transported on ice to the laboratory, frozen immediately and stored at – 80 °C until analysis. To minimize individual variance, milk was pooled together before any analysis.

3.3.2 Simulated enteral digestion of human milk in premature infants

In this study the *in vitro* digestion model incorporates both gastric and intestinal phases, based on reported luminal pH and enzyme levels, as well as transit time, observed *in vivo* in preterm infants.

Transit time, pH and pepsin concentration in the gastric phase

In the *in vivo* gastric digestion of premature infants, the pH of ingested milk is brought down by gastric HCl. Pepsin and lipase are secreted by the stomach to assist the breakdown of proteins and lipids. After gastric digestion, milk is diluted by digestive juices and the proteins and lipids in milk are partly digested. This *in vitro* digestion model was developed to mimic these gastric conditions.

In a study by Bode et al. (45), 10 preterm infants were recruited and gastric emptying was monitored. Graph 1 and Table 3 show the gastric emptying over time after feeding. The median gastric emptying half time was 1.0 hour, which was chosen as the incubating time in the gastric phase.

In a study by Omari et al. (46), the gastric pH of healthy premature infants was measured by a pH probe. As shown in Graph 2, gastric pH in premature infants was approximately 2.0 before a meal. After the meal, it climbed to around 6.5 at 30 minutes due to the dilution of milk and then declined gradually. The gastric pH was adjusted twice in this study to mimic the gradual change of gastric pH. First, the pH of human milk was adjusted to 4.0 by HCl and then incubated in 37°C shaking incubator for 30 minutes. Then, the pH of milk was brought up to 6.0 by $NaHCO_3$ and incubated for 30-minute incubation.

Martine et al. (47) measured the gastric volume and pepsin activity in premature infants after being fed human milk. According to Graph 3 and Table 4, 0.9375 FIP unit (One FIP Unit, expressed as micromoles of tyrosine equivalents liberated per minute at 25°C) pepsin was secreted to digest 1 ml human milk. It was assumed that milk was diluted 1.25 times at 30 minutes based on the fact that milk is being diluted during digestion. In this *in vitro* gastric digestion model, the pepsin activity was maintained at the 30 minutes level (0.9375 FIP unit pepsin/ ml milk). Gastric lipase was neglected in this study because of its small secretion in the stomach.

To simulate the dilution of milk by digestive juices, KCl and NaCl solutions were added to human milk (48). Diluted milk was then placed in a 37°C shaking incubator to mimic gastric peristalsis and body temperature during incubation process.

Transit time, pH and digestive enzyme concentrations in intestinal phase

In the *in vivo* intestinal digestion of premature infants, gastric digestion products are neutralized by $NaHCO_3$. Bile is secreted to emulsify lipids and pancreatin is secreted to digest carbohydrates, proteins and lipids. After intestinal digestion, milk is digested to small molecules which can easily enter enterocytes. In addition, digestive juice secreted by the small intestine makes milk further diluted.

Bode et al.(45) measured the small intestinal transit time of premaure infants using scintigraphic methods. The mean small intestinal transit time of nine premature infants was 2.1 hours. In this *in vitro* digestion model, 2.0 hours was chosen as the incubating time of the intestinal phase.

Lactose is the principle carbohydrate in human milk (49). Research conducted by Chantret et al. and Galván et al. showed that the activities of lactase in Caco-2 and HT29-ATCC cells are 0.2 and 4.4 mU/mg protein, respectively (50, 51). Shulman et al. (52) reported that activities of lactase in premature infants at an average age of ten days were approximately 10 mU/mg protein. In this study, lactase was added to breast milk to supplement the insufficient lactase secretion by co-cultures.

In the intestinal phase, pancreatin, bile and lactase were added to gastric digestion products and the pH was adjusted to 7 by $NaHCO_3$, similar to intestinal digestion conditions (48). Samples were further diluted by KCl and NaCl solution again and shaken at 37°C for two hours. The intestinal digestion was terminated by placing all the samples in a -80 °C freezer until analysis.

For the final study design, the *in vitro* digestion products were placed on the Caco-2BBE/HT29-MTX cell culture model mimicking the neonatal gut and the effects of digestion products on this cell model was studied. Because the low lactase activity of this cell model limits the entry of lactose, lactase was supplemented during intestinal digestion to compensate for this weakness (52). For more details of the *in vitro* digestion process, refer to the flow chart of *in vitro* digestion (Graph 4).

3.3.3 Caco-2BBE/HT29-MTX Cell Model Mimicking the Intestinal Mucosa

Caco-2BBE is a human colon cancer cell line, which differentiates into morphologically recognizable enterocytes with brush borders (53). In addition, it expresses fetal lactase and adult sucrase / isomaltase. Although the Caco-2BBE cell line has shown it can mimic the human enterocytes, some intrinsic characteristics make further refinement of this model desirable.

Since Caco-2BBE is derived from human colonic cells, the tight junctions of this cell line resembles more colonic epithelial cells than small intestinal epithelial cells, resulting in comparatively poor permeability for hydrophilic compounds traversing the epithelium via the aqueous paracellular pathway (54). Furthermore, the Caco-2BBE cell line is solely composed of enterocytes, whereas the human small intestine is comprised of a complex three dimensional array of tissues and cells, including enterocytes, goblet and vacuolated cells, tuft cells, lymphocytes, paneth cells, and basally-granulated cells (55). Among these cells, enterocytes and goblet cells represent the two major phenotypes in the human intestinal epithelium at the

relative proportion of 9 and 1 %, respectively. Thus, to better mimic the actual conditions of the human gut, a cell model combining both enterocytes and goblet cells was developed.

The HT-29 cell line was isolated from human colonic adenocarcinomas (56). Cell lines tend to differentiate under metabolic or biochemical pressure. Methotrexate (MTX), which inhibits dihydrofolate reductase, a key enzyme of folate cycle, can be used to induce metabolic pressure (57). The HT29-MTX cell line adapting to MTX is able to undergo differentiation and shows an exclusively mucus-secreting trait (58). This Caco2-BBE/HT29-MTX cell line can form a barrier with complex absorptive and secretory characteristics. In addition, mucin-secreting goblet cells in this cell line modulate the tight junctions and yield a mucus gel covering the whole cell surface as an additional layer, thus better mimicking physiological conditions of the human small intestine (54).

Although enterocytes and goblet cells grow at a relative proportion of 9:1 in the human small intestine, in this study, Caco-2BBE (representative of enterocytes) and HT29-MTX (representative of goblet cells) were co-cultured at the ratio of 7:3 to increase mucin production (R. Dr. Glahn, personal communication).

This Caco2-BBE and HT29-MTX cells were seeded on basement membrane Matrigel®, a reconstituted basement membrance matrix. The major components of matrigel include laminin, collagen IV, heparan sulfate proteoglycans, entactin, and nidogen. Additionally, Matrigel® contains growth factors, such as transforming growth factor-b (TGF-b), fibroblast growth factor, and tissue plasminogen activator

(59). Matrigel® has displayed its effectiveness in promoting the attachment and differentiation of both normal and transformed epithelioid cells. This cell model was placed on polycarbonate transwell chambers (Corning), which are divided into two compartments by a membrane with 0.2 μm pore. *In vitro* digested milk was added to the apical compartment; metabolic products from the Caco2-BBE/HT29-MTX monolayer, may pass from the apical to the basolateral compartment, either via paracellular mechanisms (between cells), through transcellular mechanisms such as carrier-mediated transport, or through diffusion (eg: lipid-soluble molecules).

3.3.4 Verification of Co-culture

In the current study, Caco2-BBE and HT29-MTX cells were co-cultured to mimic the intestinal mucosa of premature infant gut. To verify that this co-culture model exhibits expected characteristics, co-culture morphology and mucin secretion were examined.

Co-culture Morphology

To observe co-culture morphology, cultures grown on transwell polycarbonate filters were fixed in Karnovkey's solution, embedded in epon-araldite and sectioned on a microtome. Epon-araldite sections were stained with toluidine blue and morphology was observed under 40 X magnification (refer to the standard protocol on page 84).

Mucin Production

To measure mucin production, PAS-Schiff staining and Alcian blue staing were used. For PAS-Schiff staining, cultures were grown on Transwell polycarbonate filters, fixed in 4% paraformaldehyde (PFA), embedded using JB-4 plus® embedding kit (Polysciences) and sectioned on a microtome. Mucin was oxidized by periodic acid and stained by Schiff regent (refer to the standard protocol on page 81) (60). For Alcian blue staining, cultures were grown in petri dishes, fixed and stained. Mucin secreted on the cell surface was stained by Alcian blue and observed under 40 X magnification (refer to the standard protocol on page 83) (61).

3.3.5 Response of Co-culture to Digested Milk

Before measuring effects of milk on oxidative stress in co-culture model, cell characteristics, including monolayer barrier integrity, cell viability and adhesion, were measured after exposure of co-culture to digested milk.

Monolayer barrier integrity

After cells reach confluence, the cell monolayer confers transepithelia electrical resistance between apical and basolateral cell surfaces. When the monolayer is damaged, compromised barrier integrity leads to a drop in transepithelial electrical resistance value. Therefore transepithelial electrical resistance technique was used to measure the intactness of cell monolayer integrity (refer to the standard protocol on page 77) (62).

Cell adhesion

Cell adhesion was measured using Calcein AM (Invitrogen). Calcein AM is a non-fluorescent dye and easily permeates intact, live cells (63). Calcein AM is hydrolyzed by intracellular esterases and produces Calcein, a strongly fluorescent compound that is retained in the cell cytoplasm. The number of cells attached to the bottom is proportional to the emission of Calcein trapped in cells (refer to the standard protocol on page 86).

Cell viability

2'-7'-bis (2-carboxyethyl)-5(6)-carboxyfluorescein (BCECF AM) (Invitrogen), a cell membrane permeable dye was used to measure cell viability (64). BCECF AM easily diffuses into cells and is hydrolyzed by esterase to BCECF. BCECF is not cell membrane permeable and accumulates inside viable cells. The intensity of BCECF fluorescence is proportional to the number of viable cells (refer to the standard protocol on page 79).

To measure the ratio of live cells to dead cells, Calcein AM and Ethidium bromide were utilized. Calcein AM is a dye, which is trapped in live cells and indicates the number of viable cells by detecting its emission (63). Ethidium bromide enters cells with damaged membrane and stains nucleic acid (65). Dead cells can be counted by reading Ethidium bromide emission (refer to the standard protocol on page 85).

3.3.6 Effects of Milk on Oxidative Stress in the co-culture model

First, cells were treated with milk and oxidative stress is induced to this co-culture using hydrogen peroxide. To measure the effects of milk on reducing oxidative stress in co-culture, assays determining intracellular ROS, intracellular oxidative status, DNA damage and intracellular antioxidant enzymes were conducted.

Intracellular oxidative status

To measure the oxidative activity of the cell model, a molecular probe, 5-(and-6)-chloromethyl-2,7-dichlorodihydrofluorescein diacetate acetyl ester (CM-H_2DCFDA) (Invitrogen), was chosen. CM- H_2DCFDA is a compound, which readily diffuses into cells. Intracellularly, it is hydrolyzed by esterases to a polar non-fluorescent derivative, 2,7-dihydrodichlorofluorescin (H_2DCF). H_2DCF is retained in the cells and oxidized to the highly fluorescent compound 2, 7-dichlorofluorescein (DCF) by intracellular reactive oxygen species, such as peroxide, peroxyl radical and hydroxyl radical. By measuring the emission of DCF, the oxidative activity can be measured (refer to the standard protocol on page 78) (66).

Effects of milk on intracellular oxidative status were also monitored using dihydrorhodamine 123 (DHR) (Invitrogen). DHR is a non-fluorescent dye, which readily enters cells and is oxidized to fluorescent dye rhodamine 123 by intracellular ROS (67). The bright fluorescence emitted by rhodamine 123 upon excitation is a good indicator of intracellular oxidative status. Dihydrorhodamine 123 is specific to

superoxide ion, hydroxyl radical and hydrogen peroxide, therefore being a good supplement to CM- H_2DCFDA (refer to the standard protocol on page 95).

DNA damage

The comet assay is a rapid and sensitive technique for analysis and quantification of DNA damage (68). In this assay, cells were lysed in lysis buffer and then unwound in alkaline solution. Damaged DNA migrated from nucleus under electrophoretic conditions, forming a comet tail shape. The degree of DNA damage was determined by tail moment, which measures tail length and the fraction of DNA in the comet tail (refer to the standard protocol on page 88) (69).

Intracellular antioxidant enzymes

Intracellular antioxidant enzymes, including SOD, GPx and CAT, provides antioxidant defense against ROS attack. When cells are under attack of ROS, intracellular antioxidant enzymes are consumed. In the current study, the activity of intracellular GPx was measured (refer to the standard protocol on page 92).

3.3.7 Statistical Analysis

For each assay, one way analysis of variance (ANOVA) with the tukey post hoc test to describe relationship between means was employed and $p < 0.05$ was regarded as statistically significant.

Chapter 4 Results

4.1 Characteristics of Co-culture

4.1.1 Cell growth and morphology

Light microscopy indicates that cultures grew to confluency within 7 days. The average value of transepithelial electrical resistance was above 600, meaning tight junctions between cells are formed.

The morphology of co-culture was examined using Epon-araldite section technique. Co-culture was seeded on polycarbonate filters, fixed and embedded in epon-araldite. Figure 1 shows an Epon-araldite section stained with toluidine blue. It reveals enterocytes with the expected microvilli and brush border, as well as clusters of cells with large cytoplasmic inclusions under 40 X magnification.

Figure 1. Epon-araldite sections stained with toluidine blue

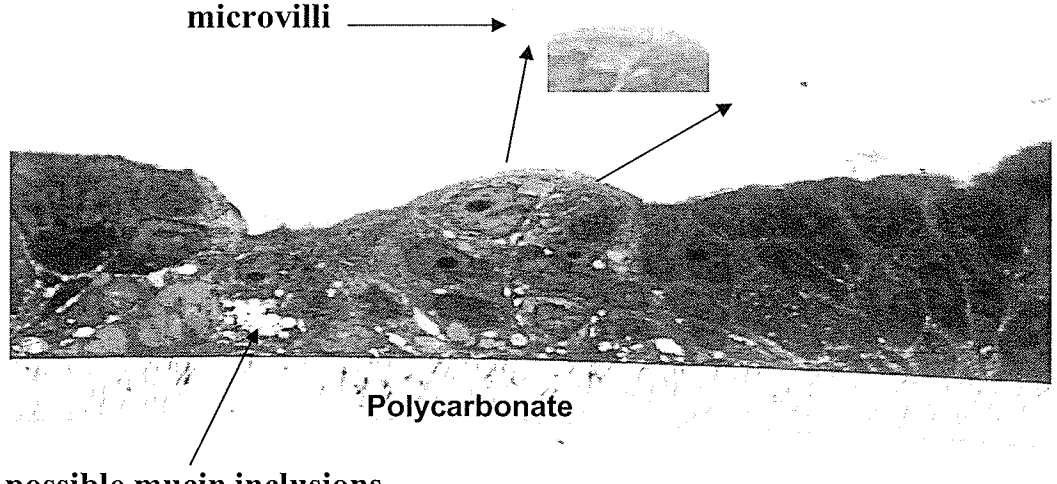

Day 21

4.1.2 Mucin secretion

4.1.2.1 Alcian blue staining

Mucin production of co-culture was determined using Alcian blue and periodic acid Schiff staining methods. Figure 2 indicates whole mount view of co-culture stained by Alcian blue. Positive Alcian blue stainning was found at day 7 and became more and more intense as time went on, indicating a progressive accumulation of mucin secretion. Staining revealed that mucin secretion reached the maximum at day 21.

4.1.2.2 PAS-Schiff staining

Figure 3 compares 12-day-old cell and 21-day-old cell sections stained by PAS-Schiff technique. In addition to a marked increase in staining intensity, a layer-shape staining was observed on the apical side of 21-day-old cell section, implying the accumulation of mucin on the surface of co-cultures.

Figure 2. Whole Mount View by Alcian Blue Staining

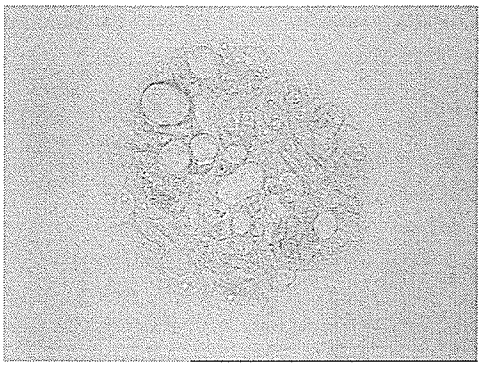

Day 7

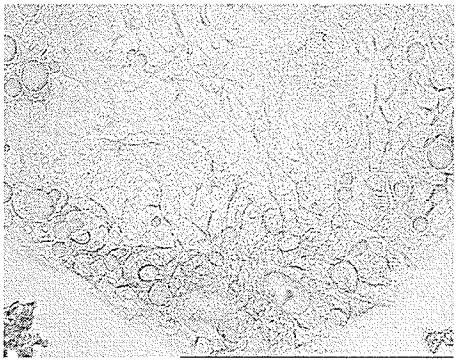

Day 9

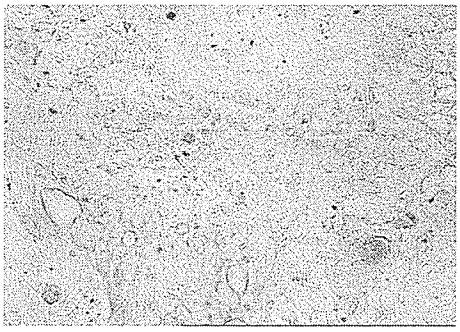

Day 12

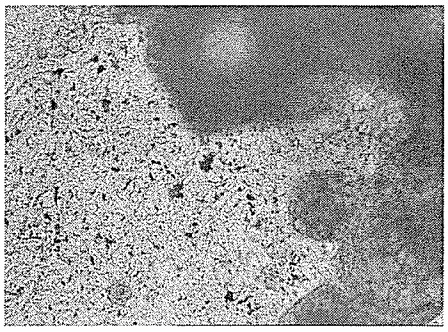

Day 15

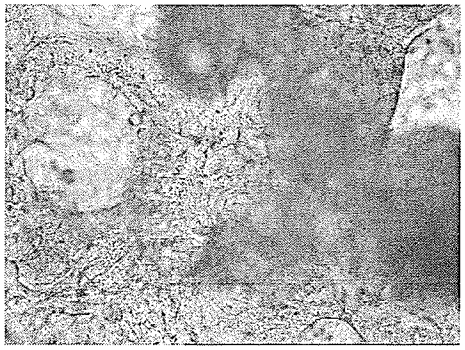

Day 18

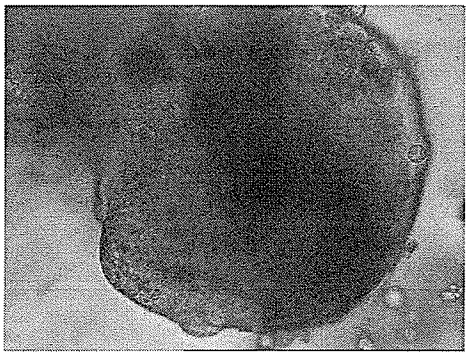

Day 21

Figure 3. JB-4 Methacrylate Thick Sections by PAS-Schiff Staining

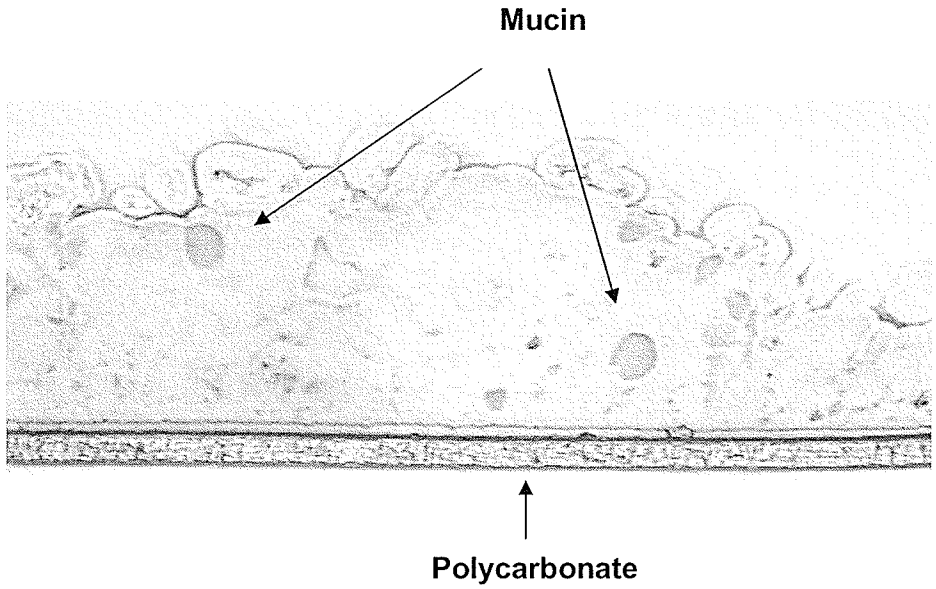

Day 12

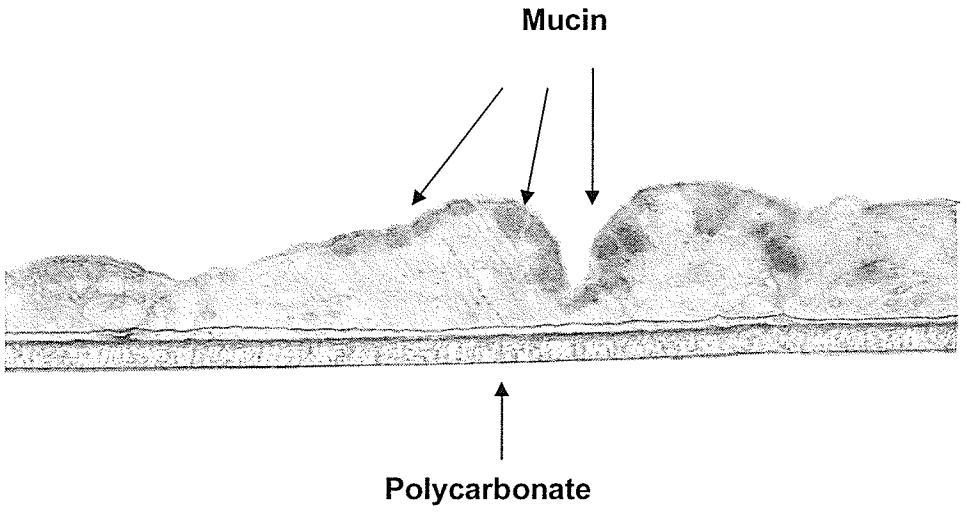

Day 21

4.2 Response of co-culture to digested milk

4.2.1 Transepithelial electrical resistance measurement

Monolayer barrier integrity during the digested milk treatment was measured by TEER. TEER was measured at baseline, 30 minutes, 60 minutes and 90 minutes after 0.5 ml of digested milk treatment. Graph 5 shows that TEER value dropped from 667.25 to 232.42 ohms after 30-minute digested milk treatment, indicating a severe damage to barrier integrity induced by digested milk. No further decrease in TEER value was observed when digested milk incubation was treated longer.

Graph 5. Effects of digested milk on cell monolayer integrity measured by TEER

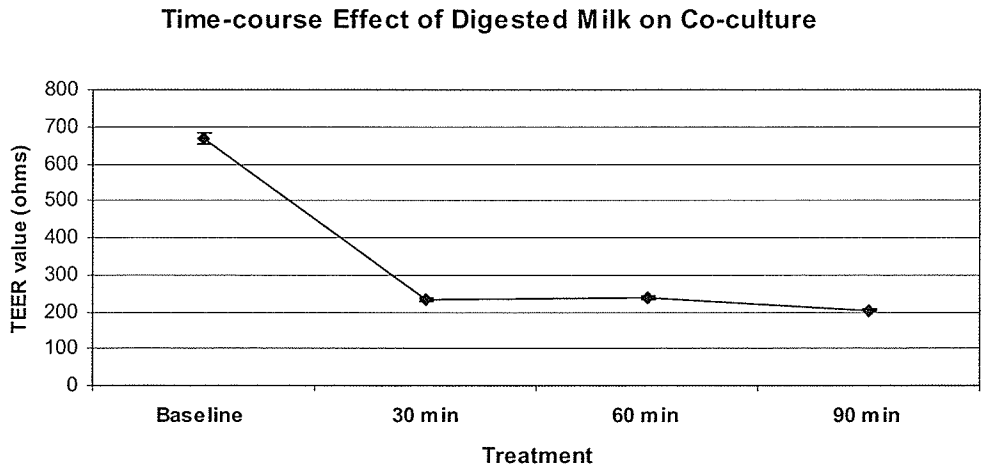

Data shown as mean+/- SEM and n=3.

4.2.2 Phenol red permeability assay

To confirm the findings from cell barrier integrity assay, permeability of co-culture to phenol red was determined. Graph 6 compares the permeability of co-culture to phenol red before and after digested milk treatment. At baseline, co-culture was treated with culture medium for three hours. Then co-culture was treated with 0.5 ml of culture medium, non-digested milk or digested milk, separately. Permeability to phenol red was measured at one hour intervals.

At baseline, permeability to phenol red was maintained steadily around 11.5 um per hour. When treated with non-digested milk and culture medium, permeability to phenol red rose to 34 uM per hour and reached a plateau afterward. When treated with digested milk for one hour, permeability to phenol red climbed to 120 uM per hour, which implies compromise of the transepithelial barrier induced by digested milk treatment.

Graph 6. Effects of digested milk on cell monolayer integrity measured by phenol red assay

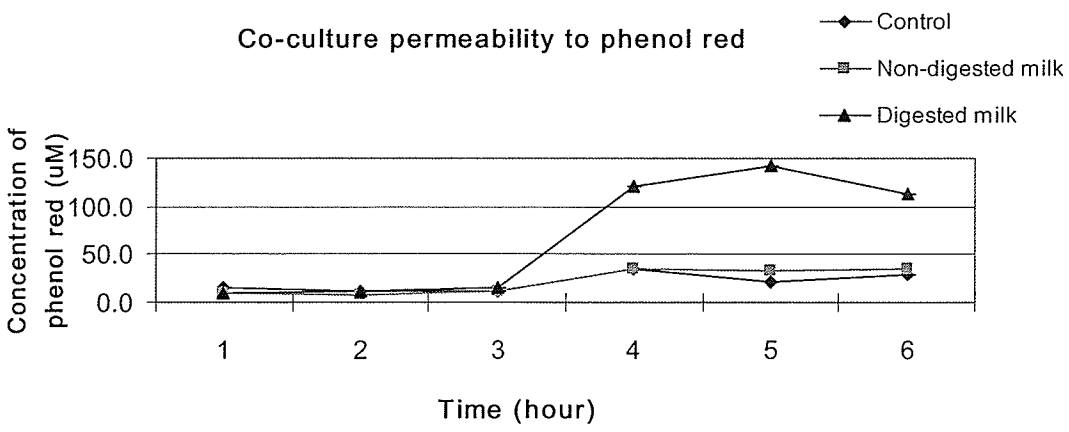

Data shown as mean+/- SEM and n=3. Statistically-significant differences ($p < 0.05$) were between digested milk and other groups at hour 4, 5, 6.

4.2.3 Cell viability

2'-7'-bis (2-carboxyethyl)-5(6)-carboxyfluorescein (BCECF AM), a fluorescent dye, was applied to measure effects of digested milk on cell viability. Co-culture was treated with 100 ul of culture medium, non-digested milk, digested milk or formaldehyde, a positive control, for 30 minutes, separately. Graph 7 shows cell viability after different treatments. Digested milk caused more cell death in comparison with non-digested milk treatment.

Graph 7. Effects of digested milk on cell viability

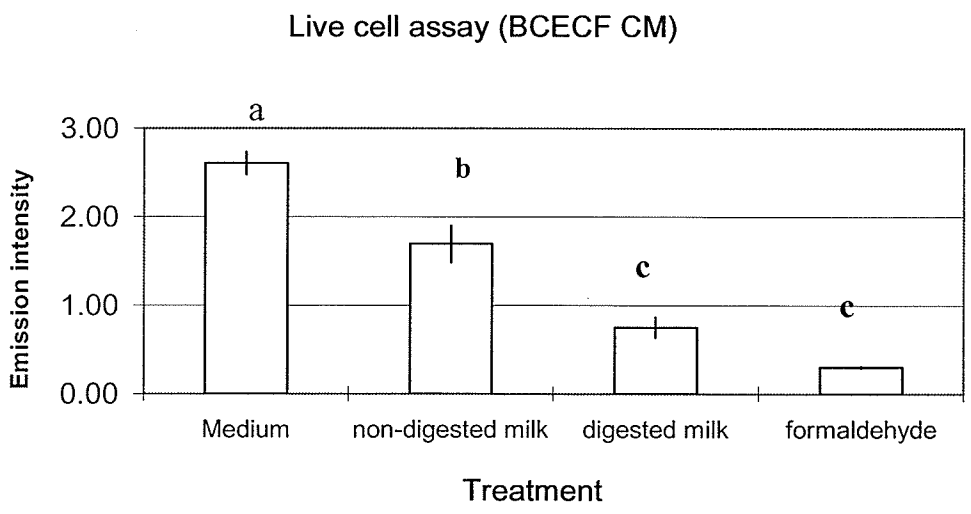

Data shown as mean+/- SEM and n=8. Different letters specify statistically-significant differences ($p < 0.05$) between groups

4.2.4 Cell adhesion

To examine effects of digested milk on cell attachment, co-cultures were treated with *in vitro* digested milk and cell adhesion was determined at different time intervals. Graph 8 depicts cell adhesion measured at different time intervals. A steep decline of cell adhesion was observed since 15- minute digested milk incubation. implying that co-cultures could only maintain their attachment for 15 minutes.

Graph 8. Effects of digested milk on cell adhesion

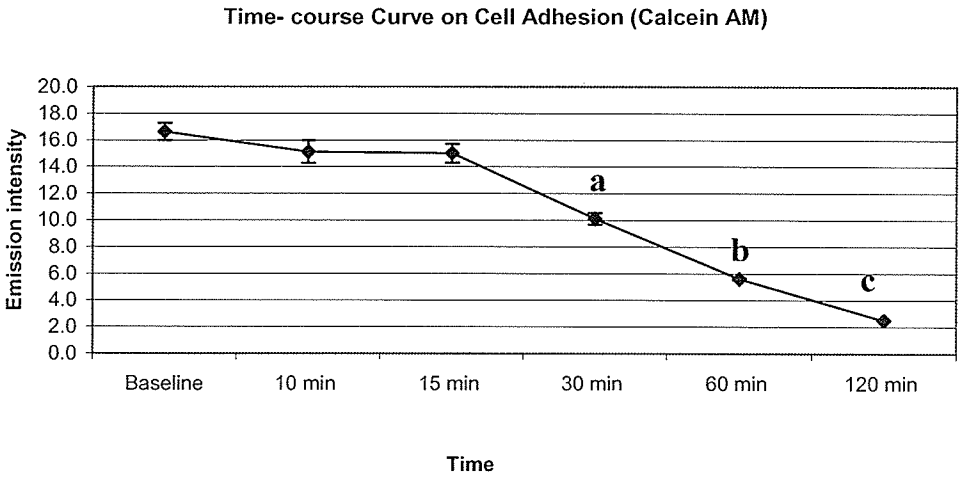

Data shown as mean+/- SEM and n=8. Different letters specify statistically-significant differences ($p < 0.05$) between time intervals

4.3 Addition of Mucin

4.3.1 Protection via exogenous mucin treatment

From previous experiments, it has been shown that barrier integrity, cell viability and cell adhesion were destroyed after digested milk treatment, likely due to digestive enzymes added in the *in vitro* digestion process. To overcome the damage caused by digestive enzymes, supplemental mucin was coated on the surface of co-culture.

The mucosa layer in human small intestines constitutes of 95% water, 3-5% (30-50 mg/mL) of mucin polycoproteins, lipids, nucleic acids, and other proteins (70). Previous study has shown that commercially supplied mucin is a relatively high in Fe and research done by Friel et al. revealed that iron supplementation might increase oxidative stress in premature infants (71). To eliminate side effects of iron on the oxidative stress measurement, chelex-100, a chelating reagent, was used to sequester metal ions in mucin.

In this study, 25 mg / ml of exogenous mucin was added to co-culture surface and protection afforded by supplemental mucin was determined according to TEER value, cell morphology, cell adhesion and cell viability assays.

4.3.2 Protective effect of added mucin on cell barrier integrity

To measure the protection of mucin on monolayer integrity, TEER was monitored. Co-culture with mucin coating or without mucin coating was incubated with culture medium or *in vitro* digested milk for 30 minutes. TEER was measured immediately after incubation with different treatments, one-hour, two-hour and three-hour recovery period.

Graph 9 shows that TEER value dropped after 30-minute 250 ul of digested milk treatment with or without mucin protection. However, TEER value restored to control group's level after two hours recovery. In contrast, TEER value of non-mucin supplementation group did not show any sign of recovery to pre-treatment levels.

Graph 9. Protective effect of added mucin on cell barrier integrity

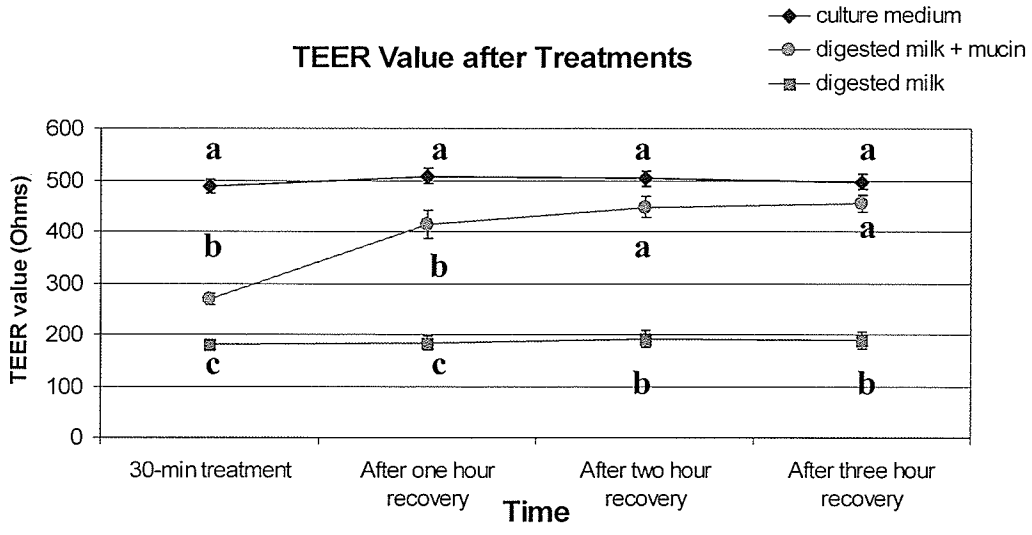

Data shown as mean+/- SEM and n=3. Different letters specify statistically significant difference ($p < 0.05$) between groups at each time point.

4.3.3 Effects of exogenous mucin on cell morphology

Protective functions of mucin against *in vitro* digested milk were also tested by examining cell morphology. Co-culture was seeded on polycarbonate filters and grown to confluence. For the mucin group, cells were coated with mucin; all the cells were incubated with culture medium or *in vitro* digested milk for 30 minutes. Post-treatment and 3-hour recovery cells were fixed, dehydrated, embedded in epon-araldite and stained with toluidine blue.

Figure 4 presents cross-sections of co-cultured cells grown on polycarbonate after different treatments. In the control group, confluent cells were closely apposed. Brush borders and were observed under 40 time objectives. In the mucin coated group, no visible damage was seen in cells fixed immediately after 30-minute *in vitro* digested milk treatment or until 3-hour recovery compared with the control group. In the non-mucin coated group, missing brush borders and a large number of highly vacuolated, detached cells were found. This finding confirmed the protection of mucin found in TEER value measurement.

Figure 4. Cross-sections of co-culture after different treatments (under 40 X magnification)

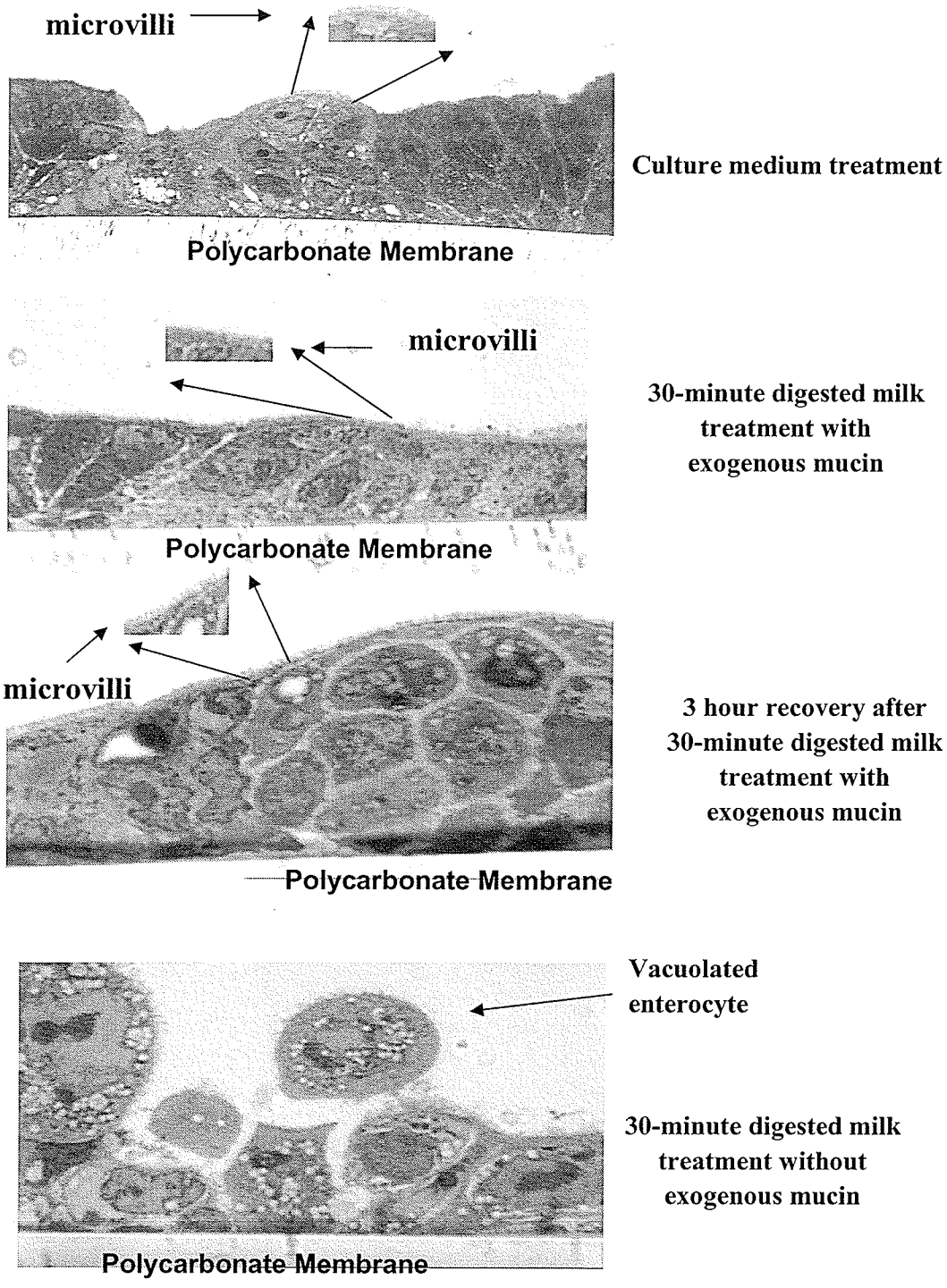

4.3.4 Effects of exogenous mucin on cell adhesion

The impact of mucin supplementation on cell adhesion was investigated by Calcein AM, a dye commonly used to determine cell adhesion. Co-culture with mucin coating or without mucin coating was treated with *in vitro* digested milk and cell adhesion was measured at different time interval.

Graph 10 compares cell adhesion after digested milk treatment with or without mucin supplementation. Results showed that mucin supplementation enabled co-cultures to withstand 30- minute digested milk treatment.

Graph 10. Effects of exogenous mucin on cell adhesion

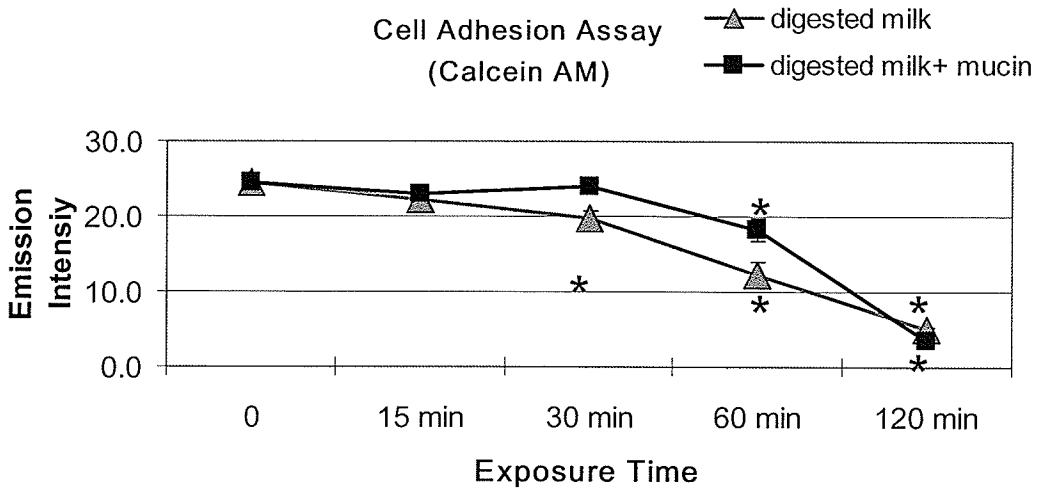

Data shown as mean+/- SEM and n=8. * Specifies statistically-significant differences ($p < 0.05$) from time 0.

4.3.5 Effects of exogenous mucin on cell viability

Mucin protection on cell viability was measured by the live dead assay. Co-culture with mucin coating or without mucin coating was treated with *in vitro* digested milk; live cells were measured using Calcein AM and dead cells were measured by Ethidium bromide.

Graph 11 shows the effects of mucin on cell viability after different treatments. Data revealed no statistically-significant differences in cell viability was seen between the control group and the 30-minute milk treatment group with exogenous mucin addition. To confirm this result, the ratio of live cells to dead cells was calculated. As shown by Graph 12, no statistically-significant difference in the ratio of live cells to dead cells was found between control and 30-minute milk treatment with exogenous mucin addition.

Graph 11. Effects of exogenous mucin on cell viability

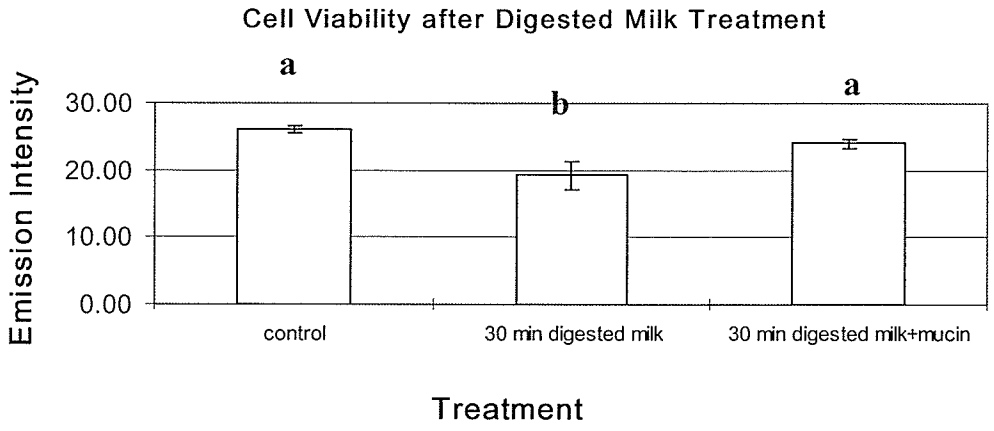

Data shown as mean+/- SEM and n=8. Different letters specify statistically-significant differences ($p < 0.05$) between groups.

Graph 12. Effects of exogenous mucin on the ratio of live cells to dead cells

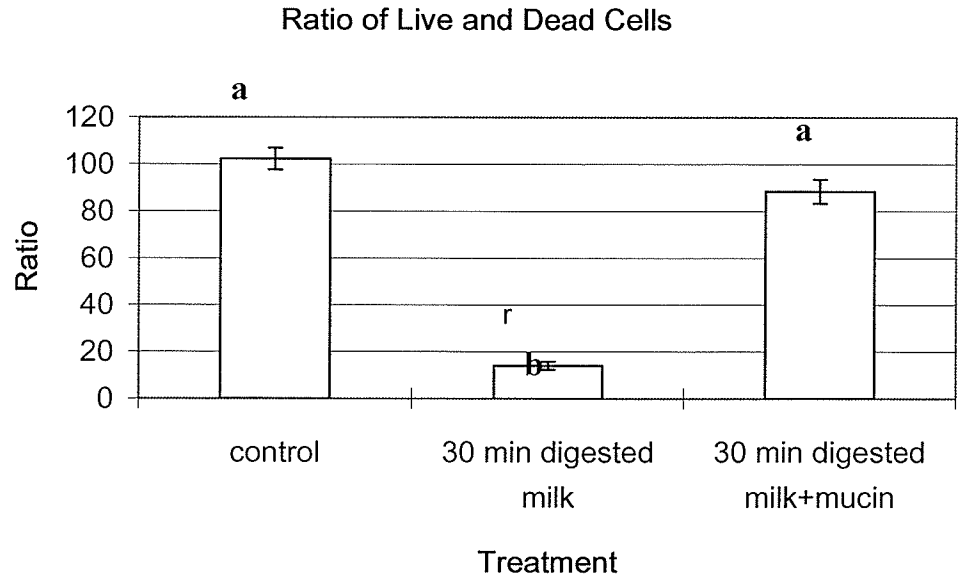

Data shown as mean+/- SEM and n=8. Different letters specify statistically-significant differences ($p < 0.05$) between groups

Taken together, our results of cell barrier integrity, cell viability and cell adhesion showed that addition of muicn enabled co-cultures to withstand 30-minute *in vitro* digested milk treatment. In the following experiments, exogenous mucin was added to co-cultures before experiments to minimize the adverse effects of *in vitro*-digested milk.

4.4 Effects of milk on oxidative stress

4.4.1 Intracellular reactive oxygen species

To measure effects of milk on oxidative stress in co-culture, cells were loaded with CM-H_2DCF, a fluorescent probe specially used for detecting intracellular reactive oxygen species. Milk samples were diluted approximately 3 times during the *in vitro* digestion process. To eliminate the dilution factor, non-digested milk was diluted 3 times before comparing its antioxidant properties with those of *in vitro* digested milk. In the following experiments, the same treatment was employed as well.1 mM hydrogen peroxide was used to induce oxidative stress and co-culture was exposed to different treatments.

Graph 13 shows effects of different treatments on intracellular oxidative stress. Non-digested milk, 3 X diluted non-digested milk, digested milk and CAT showed their effects on reducing intracellular oxidative stress compared to the positive control group.

Graph 13. Effects of different treatments on intracellular oxidative stress

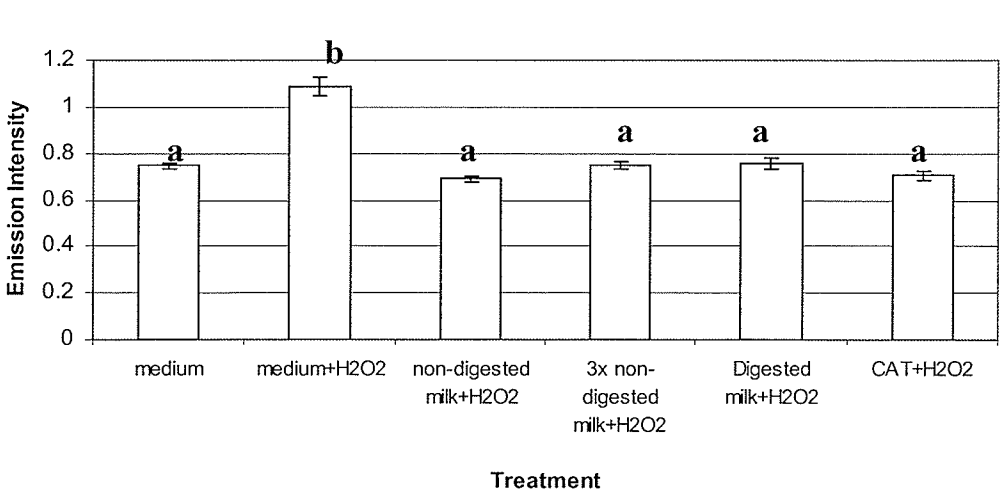

Data shown as mean+/- SEM and n=8. Different letters specify statistically-significant difference ($p < 0.05$) between groups

4.4.2 Effects of milk on intracellular oxidative status

Effects of milk on intracellular oxidative status were monitored using dihydrorhodamine 123 (DHR). DHR is a non-fluorescent dye, which readily enters cells and is oxidized to fluorescent dye rhodamine 123 by intracellular ROS (67). The fluorescence emitted by rhodamine 123 upon excitation is a good indicator of intracellular oxidative status.

In this study 1mM hydrogen peroxide was used to induce oxidative stress to co-culture after loading DHR. The co-culture was exposed to different treatments. Graph 14 shows the effects of different treatments on intracellular oxidative status. Results indicated that compared to the positive control group (medium+ 1mM hydrogen peroxide), all the treatments demonstrated antioxidant functions.

Graph 14. Effects of milk treatments on intracellular oxidative stress

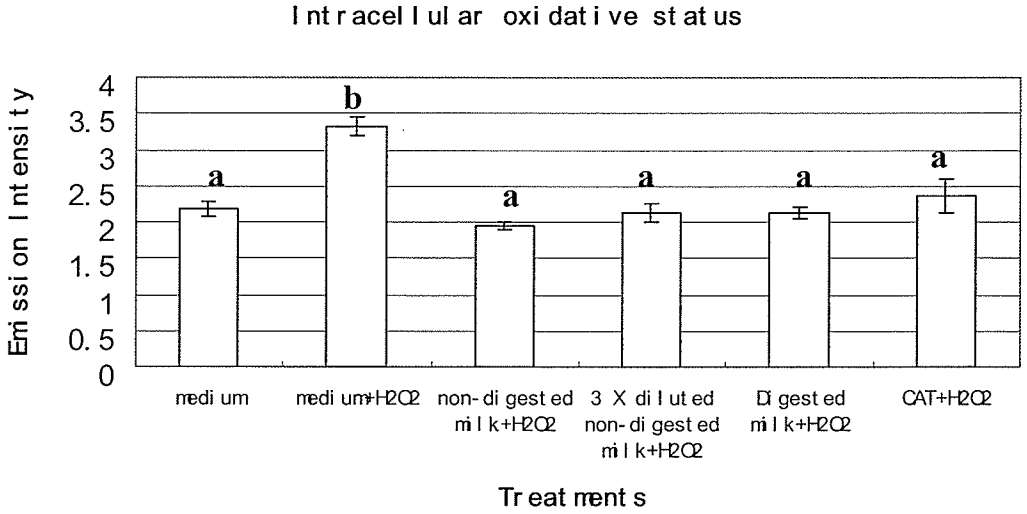

Data shown as mean+/- SEM and n=8. Different letters specify statistically-significant differences ($p < 0.05$) between groups.

4.4.3 Effects of milk on oxidative DNA damage

It is well known that excessive reactive oxygen species cause DNA damage in cells. In this assay, oxidative stress was induced by 500 um hydrogen peroxide and co-culture was incubated with different treatments.

Figure 5 depicits representatives of flurorescence micrographs of intact DNA and damaged DNA. When DNA is intact, it holds together, displaying a spheric shape. Damaged DNA migrates from nucleus by electrophoresis, forming an image like a "comet".

Graph 15 shows DNA damage calculated by tail moment after different treatments. Non-digested milk and CAT reduced DNA damaged to minimum degree among all the groups. No statistically significant differences were seen between 3 times diluted non-digested milk and digested milk in terms of capability of protecting DNA damage.

Figure 5. Intact DNA and damaged DNA

Intact DNA

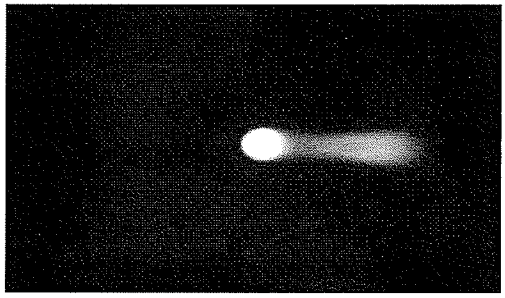

Damaged DNA

Graph 15. Effects of different treatments on DNA damage

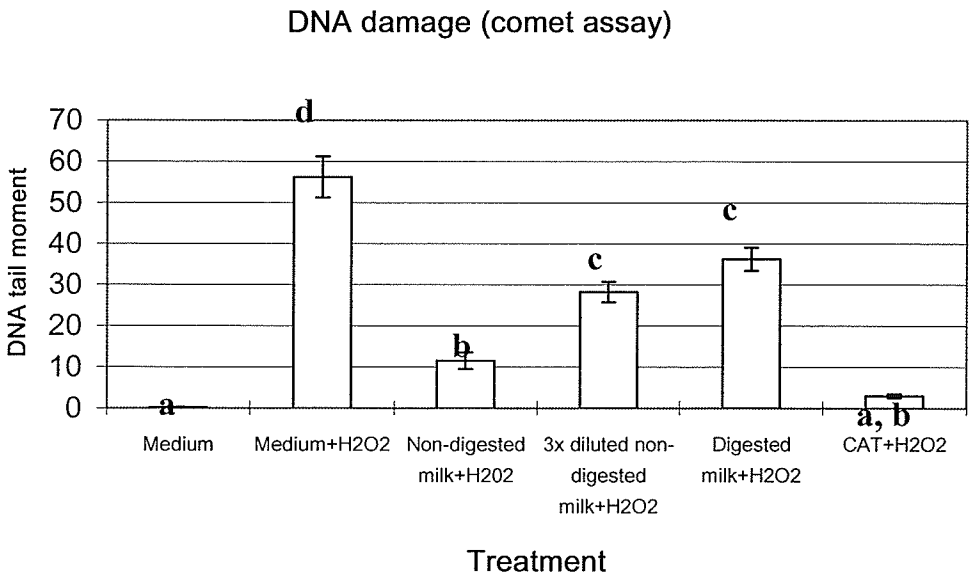

Data shown as mean+/- SEM and n=20. Different letters specify statistically-significant differences ($p < 0.05$) between groups

4.4.4 Effects of milk on GPx activities

Glutathione peroxidase (GPx) is an important antioxidant enzyme in cells. Intracellularly, it catalyzes the conversion of hydrogen peroxide to water and glutathione disulfide from glutathione (7). GPx activity is a good indicator of intracellular oxidative status.

For intracellular GPx activity measurement, co-culture was treated with 300 uM hydrogen peroxide plus different treatments for 30 minutes. After cell lysis intracellular GPx was collected and measured by GPx assay kit.

Graph 16 shows intracellular GPx activities after different treatments. No statistically-significant difference was seen between treatments except positive control.

Graph 16. Effects of different treatments on intracellular GPx activities

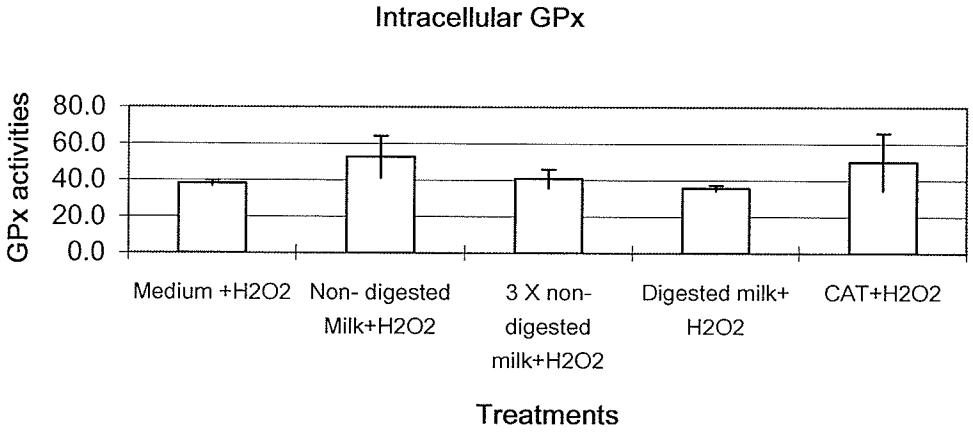

Data shown as mean+/- SEM in 800ug/ml cytoplasmic proteins. Different letters specify statistically-significant difference ($p < 0.05$) between groups

Chapter 5 Discussion

5.1 *In vitro* digestion model

Taking into account the effects of digestion on milk, *in vitro* digestion techniques are incorporated into studies by researchers. Jovani et al. (72) employed an *in vitro* digestion technique to estimate bioavailability of calcium, iron and zinc from infant formulas. For gastric digestion, the pH of formula samples was adjusted to 2.0. Three grams of pepsin solution were added and then followed by shaking at 37 °C for 2 hours. For intestinal digestion, the pH of formula samples was raised to 5 and 25 grams of pancreatin-bile extract mixture was added followed by further 2-hour incubation.

Similarly, an *in vitro* digestion technique was utilized by Etcheverry et al. (48) to study calcium, zinc, and iron bioavailabilities of fortified human milk. At the gastric stage, the pH of diluted milk samples was adjusted to 2.0 and then 0.25 mL of pepsin solution was added. Samples were placed in a 37 °C shaker for one hour. At the intestinal stage, samples were brought to pH 6 and 1.25 ml of pancreatin/bile solution was added. Samples were brought to pH 7.0, adjusted to final volume 10 ml and placed in a 37 °C shaker for two hours.

In vitro digestion techniques were employed to hydrolyze infant formulas or human milk by Jovani et al. (71) and Etcheverry et al. (50). These researchers proposed different digestive enzyme concentrations, gastric transit time and intestinal pH, but no explanation was given.

In the current study, a thorough literature search was conducted to collect data on physiological conditions of premature infant digestion. The activities of pepsin and lactase, gastric pH and gastrointestinal transit time employed in this *in vitro* digestion process were based on available data in published literature. Furthermore, the gastric pH value was readjusted to mimic the gradual change of pH in the stomach. Thus, this *in vitro* digestion model more accurately resembled the physiological conditions of premature infant digestion.

5.2 Co-culture model

Walter et al. (73) co-cultured Caco-2 cells and HT29-MTX cells to test the permeability of different drugs. In their study, HT29-MTX and Caco-2 cells were cultured at a ratio of 1:3, 1:1 or 3:1. Cell characteristics were examined by transmission (TEM) and scanning (SEM) electron microscopy; mucus secretion was examined by Alcian blue and periodic acid Schiff staining; the integrity of cell monolayer was measured via TEER value.

Their results of TEM showed sparse microvilli at the apical membrane, secretory granules fused with apical membrane and mucus released into luminal compartment. PAS-Schiff and Alcian blue staining revealed mucin secretion by HT29-MTX cells. In addition, they found that high amounts of Caco-2 cells led to high TEER values due to tighter junctions formed between Caco-2 cells.

In this study, Caco-2BBE and HT29-MTX cells were seeded at a ratio of seven to three to increase mucin production as suggested by Dr. Glahn (university of

Cornell). The characteristics of the Caco-2/HT29-MTX co-culture including cell morphology, mucin production and cell barrier integrity were examined.

Microscopy revealed that confluent cells closely apposed and attached to the polycarbonate bottom. Brush borders as well as numerous possible mucin inclusions were observed under a 40-time objective microscope. Results of Alcian blue and PAS-Schiff staining showed that a progression of mucus secretion, beginning at day seven post-seeding, and reached a maximum by day 21. The TEER value of two-week old co-culture was around 600 Ohms/cm^2. Results of this study were similar to these of the research done by Walter et al. and clearly confirmed that, in our laboratory, this co-culture model exhibits absorptive and mucin-secreting characteristics(73). These experiments also provided a basis for *in vitro* experiments wherein cultures were exposed to milk or to digested milk.

5.3 Response of co-culture to *in vitro* digested milk

The responses of this co-culture to *in vitro* digested milk were determined and some adverse phenomena were found. Data from both transepithelial electrical resistance assay and the phenol red assay showed that the monolayer barrier integrity was destroyed by *in vitro* digested milk incubation. Cell viability and cell adhesion assays showed that digested milk treatment led to significant cell death and cell detachment compared to non-digested milk treatment.

Losses of monolayer integrity, cell viability and adhesion indicated *in vitro*-digested milk negatively affected co-cultures. It was speculated that the

damage caused by the *in vitro* digested milk was due to the change of osmolality after digestion or addition of digestive enzymes. The osmolality of the *in vitro* digested milk was examined, which is similar to that of non-digested breast milk. Therefore, the loss of cells after *in vitro* digested milk was likely due to added digestive enzymes over *in vitro* digestion process.

In this study, HT29-MTX cells were incorporated to the co-culture for the purpose that the mucin secreted by HT29-MTX cells would cushion the damage by digestive enzymes. However, secreted mucin by HT29-MTX cells only formed some patchy islands, but did not constitute a whole layer. It is likely due to the fact that mucin secreted by HT29-MTX cells is not enough to protect the co-culture from digestive enzymes-induced damage. To overcome the damage caused by digestive enzymes, exogenous mucin was added to the surface of the co-culture.

5.4 Mucin supplementation

Yun et al. (74) employed an *in vitro* digestion in their study to measure the effects of ascorbic acid and polyphenolic compounds on iron bioavailability in humans. To protect cells from digestive enzymes, a 15,000 Da molecular weigh cutoff dialysis membrane was attached to an insert ring to filter digestive enzymes. To avoid the damage of digestive enzymes added in the *in vitro* digestion process, Jin et al. (70) applied 5 mg/ mL iron-depleted exogenous mucin to Caco-2 cell culture and placed 8 uM microporous membrane inserts above exogenous mucin. Jin et al. (70) found a higher iron uptake when mucin was employed in comparison with

the molecular weight cutoff dialysis membrane technique. They attributed the increase in iron uptake to the interaction between iron and mucin. In addition, mucin secreted in the human small intestine lubricates the gastrointestinal epithelium and stabilizes enzymes near the epithelial surface for nutrient hydrolysis. For these reasons, the addition of mucin was deemed a reasonable approach.

In this study, exogenous mucin was added to the co-cultures surface to minimize the damage caused by digestive enzymes. Metal ions in mucin were sequestered using a chelex-100 chelating reagent. Different concentrations of mucin were tested to determine the optimal concentration for the *in vitro* digested milk treatment. Monolayer integrity, cell microscopic morphology, cell viability and cell adhesion were used as endpoints.

No significant differences in cell viability were found between 30-minute *in vitro* digested milk treatment and the culture medium treatment after addition of 25 mg / ml mucin. Furthermore, cell adhesion was well maintained after a 30-minute *in vitro* digested milk treatment when exogenous mucin was employed. Although, exposure to *in vitro* digested milk for 30 minutes led to a decline of the TEER value compared to the culture medium treatment, suggesting *in vitro* digested milk treatment had compromised cell barrier integrity. However, TEER values returned to culture medium treated group levels in two hours, which implied that cell the monolayer integrity was restored.

Post-treatment cell morphology was examined. Longitudinal-sections of cells showed that microscopic cell structure and microvilli were well preserved after a

30-minute *in vitro* digested milk treatment when mucin was added. In contrast, cell integrity in the non-mucin supplemented group was visibly altered. Microvillar loss, cellular vacuolization and complete disruption of patches of monolayer were evident (refer to Figure 4). Taken these data together, mucin supplementation conferred a protection which enabled co-culture to withstand 30-minute *in vitro* digested milk treatment.

The *in vitro* digestion technique is widely used when bioavailability of compounds in the foods is investigated, but the adverse effects of cytolytic digestive enzymes present technical difficulties. In this study, exogenous mucin was added to the apical cell surface to effectively reduce the effects of digestive enzymes added in the *in vitro* digestion process. In comparison with previous studies, in which dialysis membrane or a combination of microporous membrane and mucin coating was adopted, the current approach is cheaper, easier to apply and physiologically closer to the *in vivo* state. Besides, villi in small intestine trap endogenous mucin, helping the accumulation of secreted mucin. Therefore, addition of exogenous mucin in the current study mimics the accumulation *in vivo*.

5.5 ROS- quenching properties of milk

Previous studies have suggested that milk has antioxidant properties. Aycicek et al. (36) compared the antioxidant power of breast milk with that of formulas. Infants aged 3-6 months were recruited for their study; 28 infants were exclusively fed with breast milk and 26 infants were exclusively fed with formula. Plasma total

antioxidant capacity, as measured by the bleaching of the characteristic color of 2, 2'-azino-bis, a stable radical cation by antioxidant, was significantly higher in the breast milk-fed group than in the formula-fed group. The measurement of plasma total peroxide is based on the principle that various plasma peroxides oxidize ferrous iron to ferric iron to form an orange complex in the presence of xylenol orange. High absorbance readings indicate elevated plasma peroxides. The researchers found higher plasma total peroxide levels in the formula-fed group. These researchers concluded that breast milk provides better antioxidant power than formula.

In the current study, effects of human milk on suppressing ROS were examined by CM-H_2DCFDA and DHR assays. Because the *in vitro* digestion process diluted milk approximately three times, non-digested human milk was diluted 3 times in the current study to exclude the dilution factor. CM-H_2DCFDA and DHR assays revealed that breast milk, 3-time diluted human milk, *in vitro* digested milk and CAT significantly alleviated oxidative stress induced by hydrogen peroxide in the co-culture.

Aycicek et al. (36) probed total antioxidant capacity and total peroxides of plasma. Their results showed that breastfeeding enhanced plasma antioxidant capacity and lowered plasma total peroxide compared with formula-feeding. In the current study, milk as well as the *in vitro* digested milk reduced ROS production in the co-culture under oxidative stress. CM-H_2DCFDA is a relatively nonselective probe that reacts with hydrogen peroxide, peroxyl radical and hydroxyl radical in the cytosolic, nuclear, mitochondrial compartments (66). Dihydrorhodamine 123 has a

broad sensitivity to superoxide, hydroxyl radical and hydrogen peroxide (75). These two assays complement each other and provide us with a broad profile of intracellular oxidative status. Furthermore, the current study first tested the effects of digested milk on quenching ROS in a mucosal epithelial model. The study by Aycicek et al. and the current study are not directly comparable given different experimental approaches, but both showed human milk possesses a unique antioxidant potential.

5.6 Effects of milk on oxidative DNA damage

Excessive production of ROS causes oxidative DNA damage, therefore the degree of DNA damage is a good indicator of oxidative status (76). The suppressive effects of breast milk on oxidative DNA damage in very low birth weight infants were examined by Shoji et al. (38). In the breast fed group, infants received more than 90% of their caloric intake as breast milk; in the formula fed group, infants received more than 90% of their intake as formulas. Urine samples were collected at 2,7,14 and 28 days of age. Urinary 8-OHdG excretion, a non-invasive marker for *in vivo* oxidative DNA damage, was determined. Their results showed that, in the breast fed group, urinary 8-OHdG excretion at 14 and 28 days of age was significantly lower than that at 2 and 7 days of age. No significant difference of urinary 8-OHdG excretion was found at different days in the formula fed group. Furthermore, urinary 8-OHdG excretion at 14 and 28 days of age was significantly lower in the breast fed group than that in the formula fed group.

In the current study, DNA damage in cells was investigated by the comet assay. Results indicated that non-digested milk and CAT most effectively alleviated DNA damage induced by hydrogen peroxide among all the groups. 3-time diluted non-digested milk and digested milk showed less efficiency in preventing DNA damage.

The clinical trial conducted by Shoji et al. (38) found less oxidative DNA damage in the breast-fed group compared to the formula-fed group. This study indicated breast milk was more effective in suppressing oxidative DNA damage than 3-time diluted milk and *in vitro* digested milk. It is speculated that dilution caused the loss of antioxidant properties of 3-time diluted milk. In addition to the dilution factor, the antioxidant properties of *in vitro* digested milk may also be compromised by the *in vitro* digestion process, which probably destroyed antioxidant compounds and brought in digestive enzymes with DNA-destructive potential.

8-OhdG, an oxidized nucleoside of DNA, is excreted in the urine upon DNA damage (77). It is a biomarker of cellular oxidative stress and is commonly used to detect DNA lesion in clinical studies. In Shoji et al.'s clinical trial, urinary 8-OhdG was chosen to estimate oxidative DNA damage in infants. In comparison, the comet assay is a rapid, sensitive and relatively low-cost technique widely used to detect DNA damage in single cells (78). Thus it was adopted in this study to estimate effects of human milk on DNA damage in the co-culture cell model. Shoji et al.'s clinical trial, in conjunction with the current study, indicated that milk reduces oxidative DNA damage *in vivo* and *in vitro*.

5.7 Effects of milk on intracellular antioxidant enzymes

Shoji et al. (9) compared antioxidant properties of breast milk with those of bovine milk and infant formulas using intestinal epithelial IEC-6 cells. In their study, human colostrum samples, bovine milk and commercial formulas were first defatted by centrifuging twice at 3,000 g for 30 minutes and then diluted 100 times in DMEM. To measure antioxidant properties of human milk, IEC-6 cells were pre-incubated with 100-fold diluted defatted human colostrum, bovine milk or formulas for 24 hours and intracellular activities of CAT and SOD were measured by a commercial spectophotometric method and election spin resonance technique, respectively. Shoji et al. hypothesized that IEC-6 cells absorb antioxidant enzymes in human milk or human milk promotes production of these enzymes (9). No significant differences were observed between the control group and the 24-hour human milk incubation group.

In comparison, the activity of intracellular GPx in the current study was determined by commercial GPx assay kit. Co-cultures were treated with culture medium, breast milk, 3-time diluted breast milk or *in vitro* digested milk for 30 minutes. Oxidative stress was induced using one mM hydrogen peroxide. Intracellular GPx was extracted from cells and its activities were measured by a commercial kit. Based on the hypothesis that induced oxidation consumes intracellular GPx, we expected that milk would quench induced ROS, therefore

preserving intracellular GPx. However, no differences in GPx activities were seen after treatment in all the groups.

In Shoji's study (9), milk pre-incubation did not result in a difference of intracellular antioxidant enzymes. It is possible that milk samples were too diluted to lead to any significant change of CAT and SOD. Also, the removal of fats prior to the experiment may affect the uptake and production of intracellular CAT and SOD. Similarly, in the current study, no significant differences of GPx were found between each group. The possible explanation is that in the current study no blank control group was designed to compare with other treatments. Further studies are needed to investigate the effects of milk on intracellular antioxidant enzymes.

5.8 Study strength

1. Introduction of co-culture for *in vitro* digested milk treatment

In previous studies, IEC-6 cells or Caco-2 cells were used to test the properties of human milk (9, 79). In this study, a Caco-2BBE/ HT29-MTX co-culture was adopted. This co-culture cell model exhibits absorptive and secretory characteristics that closely mimic the neonatal epithelium. Furthermore, this co-culture was grown on Matrigel®, an artificial basement membrance matrix promoting attachment and differentiation of cells, therefore closely simulating the *in vivo* arrangement of the mucosal eithelium.

To verify that this co-culture is an appropriate model to test the antioxidant properties of *in vitro* digested breast milk, the response of this co-culture to *in vitro*

digested breast milk was examined. Results of cell viability, cell attachment, cell morphology and barrier integrity showed that addition of mucin enabled this co-culture to maintain its characteristics after a 30-minute *in vitro* digested milk treatment. To our knowledge, this co-culture model is the first used to test antioxidant properties of *in vitro* digested breast milk.

2. Usage of the *in vitro* digestion

In vitro digestion techniques have been widely used for testing properties of foods. Researchers have employed *in vitro* techniques to digest human milk or infant formulas, but the *in vitro* conditions they designed did not closely reflect the *in vivo* state of infants.

In this study, the *in vitro* digestion process employed was based on reported pH, digestive enzyme activities and gastrointestinal transit time of preterm infants. Moreover, gastric pH was readjusted to follow the changing pattern of pH in the stomach. Therefore, compared to the other *in vitro* techniques used to digest human milk, this *in vitro* digestion physiologically more accurately reflects premature infant digestion.

3. Application of mucin to the co-culture

In this study, exogenous mucin was added to the co-culture to protect cells from being damaged by still-active digestive enzymes. Compared to previous studies, which used dialysis or heating to exclude the damage resulted from digestive enzymes, addition of mucin not only buffers the damage caused by digestive enzymes, but also creates a microenvironment close to the *in vivo* mucosa (80, 81).

4. Analytical methods probing intracellular oxidative status

In previous studies, analytical methods, such as FOX-2 assay and TBARS assay, were used to determine different oxidative end products in human milk (71). In this study, CM-H_2DCFDA assay and DHR assay measure intracellular oxidative status, which is physiologically closer to the *in vivo* states. Furthermore, as both dyes were relatively non-selective to ROS, they provided a more comprehensive profile of the intracellular oxidative status.

5.9 Study limitations

1. Cultured cells do not behave as they would *in vivo*.

In this study, transformed cells, Caco-2BBE and HT29-MTX cells, were utilized. These transformed cells have lost some characteristics found in primary cells due to mutation. In addition, the human small intestine is a three dimensional, complex tissue and comprised of various cells, including enterocytes, goblet and vacuolated cells, tuft cells, lymphocytes, paneth cells, and basally-granulated cells (55). This cell culture model does not fully reflect the characteristics *in vivo*.

To overcome this, a Caco-2BBE/HT29-MTX cell model, which consist of enterocytes and goblet cells, the two major cells in the human small intestine, was used. Mucin secreted by HT-29MTX cells and exogenous mucin provide a mucus layer which is much more representative of the mucosal microenvironment *in vivo*. The Caco-2BBE subclone expresses both adult and fetal phenotypes, thus better approximating the neonatal gut. This model can form a barrier with absorptive and

secretive features, which functions more like the actual human gut. Furthermore, co-culture was grown on Matrigel substrate that promotes cell growth, attachment and differentiation, and is also more representative of the *in vivo* states.

This cell culture is easy to be control and observe compared to animal research and clinical trials. Moreover, this model is relatively low-cost and not complicated by ethical issues.

2. *In vitro* digestion can not represent *in vivo* digestion

Digestion is a complex and dynamic process, in which digestive enzymes, hormones and fluid work synergistically to break food down to absorbable molecules. The *in vitro* digestion process used in this study can not completely mimic the sophisticated *in vivo* digestion.

To closely simulate the *in vivo* digestion of premature infants, the *in vitro* digestion process in this study was based on available reported pH, enzyme activities and transit time of preterm infant digestion. In addition, gastric pH was readjusted in this study to simulate the constant change of pH in the stomach.

3. Exogenous mucin was added to the co-culture to overcome *in vitro* digested milk-induced damage.

In this study, HT29-MTX cells were incorporated into the co-culture to create a mucin layer, which can protect cells from being damaged by digestive enzymes. However, results indicated that *in vitro* digested milk treatment caused losses of cell viability, cell adhesion and barrier integrity, implying that mucin produced by

HT29-MTX cells was not sufficient to resist the *in vitro* digested milk-induced harm.

To overcome these side effects, exogenous mucin was applied to co-culture in the current study to mimic the *in vivo* microenvironment, in which secreted mucin is trapped in villi. Compared to previous studies, in which digestive enzymes were heated or dialyzed, addition of exogenous mucin in the current study is more physically relevant (80, 81).

5.10 Summary

An *in vitro* digestion process simulating premature infant digestion was developed in this study. Based on available published pH, enzyme concentrations and transit time, this refined *in vitro* digestion process more closely mimics the *in vivo* digestion of preterm infants than previous techniques.

A Caco-2BBE/ HT29-MTX cell culture was established to model the neonatal intestine. Morphological observations and mucin-staining techniques indicated that this co-culture cell model resembles absorptive and mucin-secreting features of neonatal epithelium.

The applicability of the co-culture model to *in vitro* digested milk sample was tested. Bioassays showed that direct exposure of this model to *in vitro* digested milk resulted in losses of cell viability, cell adhesion and cell barrier integrity. The same assays showed that supplementation of exogenous mucin enabled this co-culture model to withstand a 30-min incubation of *in vitro* digested milk. The average

intestinal transit time of human milk in premature infants was 2 hours based on study by Bode et al.(45). However, the two-hour transit time was the time that milk moved from duodenum to ileum. Thus 30 minutes was deemed sufficient to mimic conditions found in the human neonatal intestine.

In the current study, it showed that *in vitro*- digested milk reduced oxidative stress in the co-culture model. Our results confirmed the previous findings that breast milk decreases oxidative stress in a physiological system. The results of the CM-H_2DCFCA and DHR assays indicated that human milk and *in vitro* digested milk are equally efficient in reducing the formation of intracellular ROS in the co-culture. The comet assay showed that *in vitro* digested milk has less efficiency in decreasing oxidative DNA damage than breast milk, likely due to the dilution or compromise of antioxidant compounds during *in vitro* digestion process.

5.11 Directions for future research

The current study utilized a refined cell culture model and an *in vitro* digestion process to test the effects of human milk on oxidative stress. Although the cell culture model and the *in vitro* digestion used in this study were designed to simulate the physiological conditions in premature infants, it still does not completely reflect the *in vivo* states. Animal research and clinical studies are expected to be conducted to examine the antioxidant properties of breast milk *in vivo*.

It is known that milk contains a variety of antioxidant compounds. However, many antioxidant compounds are still not identified and their mechanism remains

unknown. In future studies, compounds with specific antioxidant potential need to be identified. Compounds, whose antioxidant properties identified by chemical methods, can be tested on this cell culture model to examine their physiological antioxidant properties.

The mechanisms as to how specific antioxidant compounds in milk exert these properties in our body are fully understood. Molecular studies investigating antioxidant compounds in human milk will make manufacturing artificial antioxidant compounds possible.

List of Tables

Table 1. Potential Diseases of Premature Infants

Undernutrition	Asphyxia
Anemia	Respiratory distress syndrome
Retinopathy of prematurity	Unconditioned suck and swallow
Poor temperature control	Hyperbilirubinemia
Apnea	Hypocalcemia
Glucose intolerance	Periventricular leukomalacia
Necrotizing enterocolitis	Infection
Intraventricular hemorrhage	Fat malabsorption
Decreased gastric motility	Limited renal function
Osteopenia	Hypotension
Patent ductus arteriosus	Bronchopulmonary dysplasia

(Table 1 is taken from Anderson DM 2004 Nutrition of Premature Infants.)

Table 2. Main nutrients in 100 ml human breast milk

Protein, g	0.9	Sodium, mg	11.2-14
Fat, g	3-5	Vitamin D, IU	2.5-5.0
Carbohydrate, g	7.3	Vitamin E, IU	0.48
Calcium, mg	29.4	Vitamin C, mg	5.0-6.0
Biotin ,ug	0.53	Vitamin A, IU	133-177
Magnesium, mg	3.0	Vitamin B6, ug	31.0-50
Iron, mg	0.02-0.04	Vitamin B12, ug	0.02-0.06
Zinc, mg	0.15-0.25	Nicotinic acid, ug	0.18
Copper, ug	31	Folic Acid, ug	4.2-5.0
Chloride, mg	37.3	Phosphorus, mg	13.9
Potassium, mg	44.3	Pantothenic Acid ug	261

(Table 2 is from Anderson DM 2004 Nutrition of Premature infants.)

Table 3. Gastric emptying time of premature infants

Patient no.	Gastric emptying half time $T_{½GE}$ (hours)	Residual gastric activity $R_{(1h)}$ (percent)	Residual gastric activity $R_{(2h)}$ (percent)	Orocecal transit time OCTT (hours)
1	–	21	6	1.3
2	0.5	31	16	2.3
3	1.0	34	24	2.9
4	2.0	54	40	5.4
5	1.2	65	24	3.4
6	0.6	19	15	3.1
7	3.0	100	61	>12
8	0.8	40	22	5.4
9	0.5	35	13	2.2
10	1.6	71	28	6.1
Median	1.0	37.5	23	3.1
Maximum	3.0	100	61	6.1
Minimum	0.5	19	6	1.3

(Table 3 is taken from Bode S, Dreyer M, Greisen G 2004 Gastric emptying and small intestinal transit time in preterm infants: a scintigraphic method. Pediatr Gastroenterol Nutr 39:378-382.)

Table 4. Clinical data of infants

Group	Human milk* (n = 11)	SMA† (n = 9)	Similac‡ (n = 8)
At birth			
Gestational age (wk)	29.5 ± 0.6 (26–32)	29.1 ± 0.9 (25–32)	28.9 ± 1.4 (24–34)
Weight (kg)	1.18 ± 0.07 (0.63–1.60)	1.09 ± 0.09 (0.66–1.60)	1.00 ± 0.14 (0.49–1.69)
Head circumference (cm)	27.5 ± 0.7 (26–31)	24.5 ± 0.5 (24–32)	26.3 ± 1.4 (22–32)
Length (cm)	37.2 ± 1.9 (23–41)	35.3 ± 1.3 (30–43)	37.0 ± 1.8 (31–43)
At start of study			
Age (wk)	5.5 ± 0.7 (1–9)	4.6 ± 0.9 (1–8)	5.8 ± 1.4 (1–11)
Weight (kg)	1.49 ± 0.06 (1.3–1.8)	1.41 ± 0.06 (1.2–1.8)	1.36 ± 0.07 (1.1–1.8)
Head circumference (cm)	30.6 ± 0.3 (28–32)	28.7 ± 0.4 (27–33)	29.4 ± 0.7 (27–32)
Length (cm)	42.3 ± 0.9 (38–46)	40.1 ± 0.9 (37–47)	40.7 ± 0.8 (38–44)
At end of study			
Age (wk)	7.5 ± 1.3 (3–13)	7.0 ± 0.9 (3–13)	7.4 ± 0.9 (4–12)
Weight (kg)	1.7 ± 0.09 (1.4–2.2)	1.6 ± 0.05 (1.4–1.8)	1.5 ± 0.08 (1.2–1.8)
Head circumference (cm)	31.2 ± 0.5 (29–34)	30.8 ± 0.8 (28–35)	30.0 ± 0.7 (27–32)
Length (cm)	42.5 ± 0.7 (41–47)	41.9 ± 0.5 (40–47)	41.5 ± 0.7 (40–47)
No. of tests	2.1 ± 0.4 (1–5)	2.3 ± 0.5 (1–5)	1.6 ± 0.3 (1–3)

Data are means ± SEM and ranges (parentheses).

* Milk of mothers.

† SMA Super Preemie formula.

‡ Similac Special Care 20–24 kcal/oz.

(Table 4 is taken from Armand M, Hamosh M, Mehta NR, Angelus PA, Philpott JR, Henderson TR, Dwyer NK, Lairon D, Hamosh P 1996 Effect of human milk or formula on gastric function and fat digestion in the premature infant. Pediatr Res 40:429-437.)

List of Graphs

Graph 1. Time-activity curves for gastric emptying in premature infants

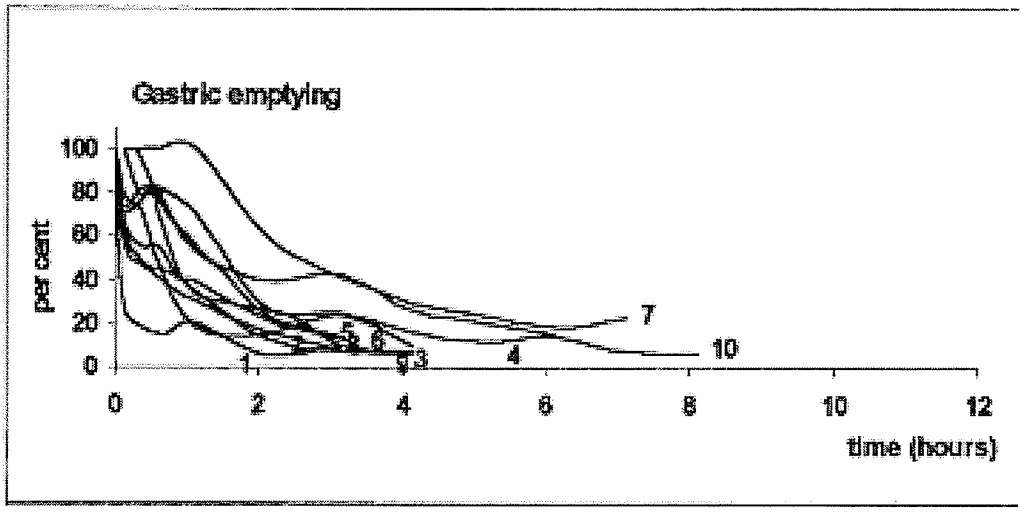

(Graph 1 is taken from Bode S, Dreyer M, Greisen G 2004 Gastric emptying and small intestinal transit time in preterm infants: a scintigraphic method. Pediatr Gastroenterol Nutr 39:378-382.)

Graph 2. Gastric pH profile in premature infants after feeding milk

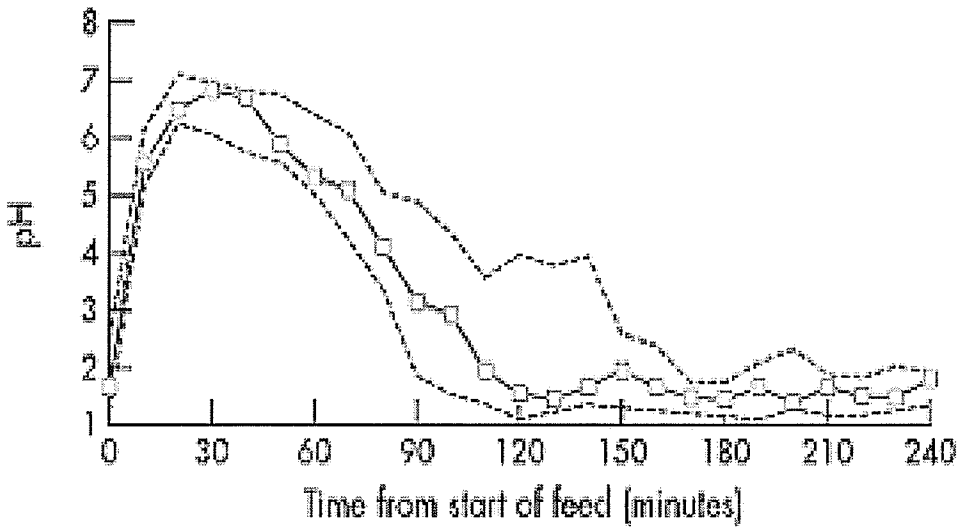

(Graph 2 is taken from Omari TI, Davidson GP 2003 Multipoint measurement of intragastric pH in healthy preterm infants. Arch Dis Child Fetal Neonatal Ed 88:F517-520.)

Graph 3. Time-pepsin activity in premature infants

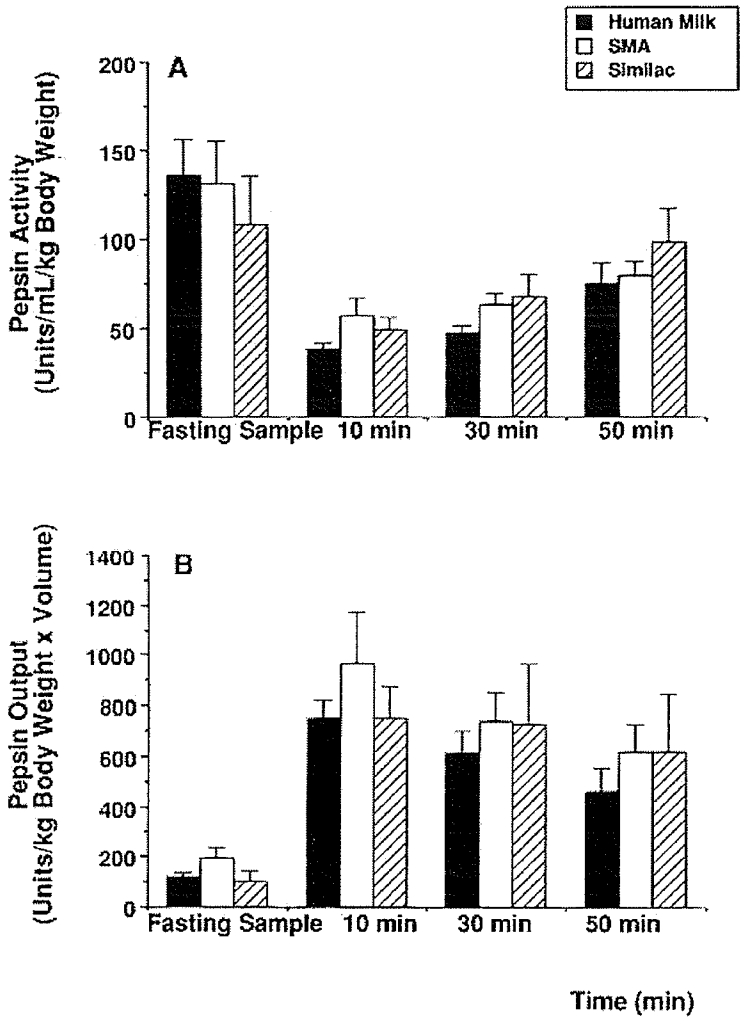

(Graph 3 is taken from Armand M, Hamosh M, Mehta NR, Angelus PA, Philpott JR, Henderson TR, Dwyer NK, Lairon D, Hamosh P 1996 Effect of human milk or formula on gastric function and fat digestion in the premature infant. Pediatr Res 40:429-437.)

Graph 4. Flow chart of the *in vitro* digestion procedure

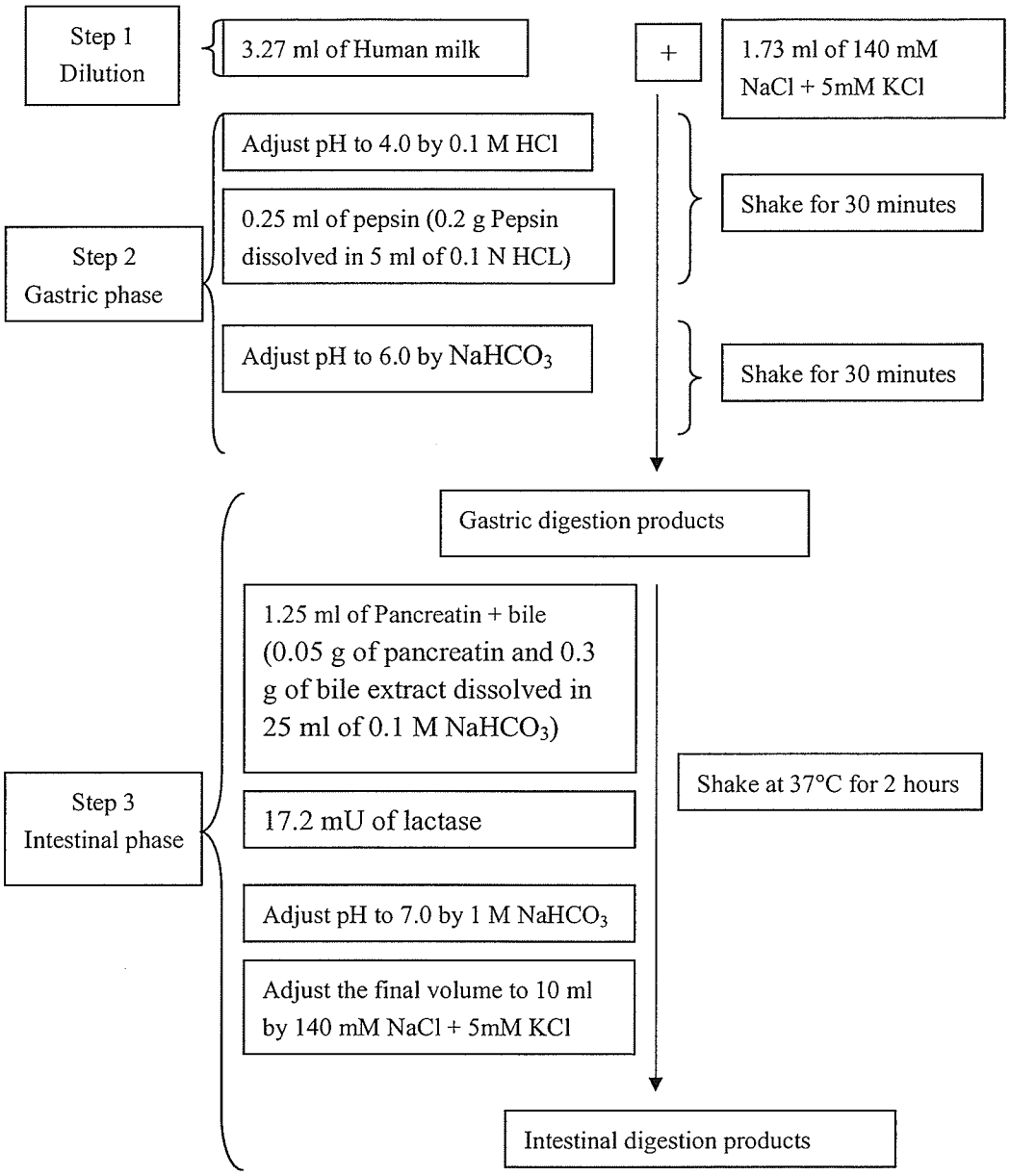

Appendix standard protocol of experimental methods

Seeding co-culture

Purpose:

Prepare co-cultures for further experiments

Material:

Caco-2BBE cells (ATCC), HT29-MTX cells (donated by Dr. Thomas Kissel [University of Marburg] and Per Artursson [University of Lund)], 500 ml Dulbecco's Modified Eagle's Medium (Gibco) supplemented with 5ml 100 U/ml penicillin/ 100 μg/ml streptomycin solution, 10 ml 2 mM L-glutamine solution, 5 ml 1 mM sodium pyruvate solution, 5 ml 10 μg/ml human transferring solution, and 60 ml 10% fetal bovine serum, EDTA, trypsin, plates pre-coated with matrigel

Procedure:

1. Caco-2BBE cells and HT29-MTX cells are maintained in an incubator, which is maintained at 37°C, an atmosphere of 5% CO2 and 95% air and 80% humidity. Supplemented culture medium is changed every 2 days until cells grow to confluence.
2. Transfer one flask of Caco-2BBE cells and one flask of HT29-MTX cells to a sterile hood.
3. Aspirate old medium, add 1 ml EDTA to each flask and shake flasks gently.
4. Aspirate EDTA and add 1 ml EDTA and 1.5 ml trypsin to each flask.
5. Incubate cells in the incubator until most of cells fall off from the bottom.

6. Wash all the cells off from the bottom with culture medium and transfer to tubes.

7. Spin cells down, aspirate culture medium and resuspend cells.

8. Pipette 10 ul homogenized cells onto the notch of the hemocytometer covered by a coverslide.

9. Count the total number of cells in a diagonal frames with sixteen grids and average it.

10. Mix Caco-2BBE cells and HT29-MTX cells at a ratio of 7:3 and seed cells in plates pre-coated with matrigel.

Matrigel preparation

Purpose:

Coat plates with matrigel to enhance cell attachment and differentiation.

Material:

Matrigel © Matrix (BD Biosciences), Dulbecco's Modified Eagle's Medium (Gibco)

Procedure:

1. Thaw aliquoted matrigel in 4 °C fridge overnight.

2. Transfer matrigel to sterilized hood on ice.

3. Dissolve matrigel in non-serum culture medium to certain concentration, as soon as possible (in this study 1% matrigel is used).

4. Coat each well of the plate with matrigel (recommended amounts for different plates are listed below: each petri dish is coated with 1 ml matrigel; each well of

multiwell plates is coated with 0.5 ml matrigel; each well of 96-well black wall plates is coated with 50 ul matrigel; each well of transwell is coated with 170 ul matrigel).

5. Plates are ready for cell seeding after one hour incubation.

Transepithelial electrical resistance (TEER)

Purpose:

Examine monolayer barrier integrity by measuring transepithelial electrical resistance.

Material:

Transwell © polycarbonate filters (Corning), REMS autosampler

Principle:

When epithelial cells grow confluent, they form a tight monolayer barrier, which acts as a boundary (82). This barrier is maintained by the formation of intercellular junctions between neighboring cells. The integrity of intracellular junctions is responsible for the movement of small molecules, such as ions and nutrients, via the paracellular route. Thus, the permeability of a cell monolayer can be indirectly examined by testing monolayer integrity.

The measurement of transepithelial electrical resistance is able to determine the resistance across the tight junctions (62). Loose intracellular junctions lead to a drop of transepithelial electrical resistance value. Therefore transepithelial electrical

resistance technique can be used to measure the intactness of cell monolayer integrity.

Procedure:

Precaution: electricity conductivity is affected by the temperature of fluid, therefore assuring the temperature of fluid constant at each measurement.

1. Grow cells on polycarbonate membranes with 0.4um pore size in 12 diameter transwell until cell confluence.
2. Measure the initial transepithelial electrical resistances values using REMS autosampler.
3. Choose option plate 1 Li 12 well, table display total resistence and click start.
4. Aspirate medium and add experimental solution for experiment groups.
5. Aspirate experimental solution after incubation and measure transepithelial electrical resistances values by following step 2, 3.

Intracellular oxidative stress (CM- H_2DCFDA)

Purpose:

Monitor intracellular oxidative stress state by measure the production of intracellular reactive species.

Principle:

To measure the oxidative activity of the cell model, a molecular probe, 5-(and-6)-chloromethyl-2, 7-dichlorodihydrofluorescein diacetate acetyl ester (CM-

H_2DCFDA), will be employed. CM- H_2DCFDA is a non-polar compound, which can readily diffuse into cells. Intracellularly, it is hydrolyzed by esterases to a polar non-fluorescent derivative, 2, 7-dihydrodichlorofluorescin (H_2DCF). H2DCF is trapped in the cells and oxidized to the highly fluorescent compound

2,7-dichlorofluorescein (DCF) by intracellular reactive oxygen species. By measuring the emission of DCF, the oxidative activity can be measured (66).

Materials:

CM-H_2DCFDA, PBS, H_2O_2.

Procedure:

1. Add 100 uL of 10uM CM-H_2DCFDA to each well.
2. Aspirate dye after incubation for 30 minutes and wash with PBS 3 times.
3. For positive control, add 1mM H_2O_2.
4. Aspirate after incubation for 30 minutes and wash with PBS 3 times.
5. Go to toolbar session and choose template li under new session.
6. Go to area definition and highlight region to be measured.
7. Go to toolbar steps and choose measure.
8. Choose 485/527nM filter pair and click measure from steps.
9. Save data from toolbar sheet.
10. Intracellular redox potential is proportional to emission detected at 527 nM

.

Cell viability assay

Purpose:

Measure cell viability after treatments

Principle:

2'-7'-bis (2-carboxyethyl)-5(6)-carboxyfluorescein (BCECF AM) (Invitrogen) readily diffuses into cells. Inside cells it is hydrolyzed by intracellular esterase to BCECF. BCECF is not cell membrane permeable and is retained inside viable cells. The intensity of fluorescence emitted by BCECF is proportional to the number of viable cells.

Materials:

BCECF AM, PBS

Procedure:

For the cell viability assay, the co-culture is grown in 96 black well

1. Add 100 uL of 10 uM BCECF AM to each well after treatment.
2. Aspirate dye after incubation for 30 minutes and wash with PBS 3 times.
3. Go to toolbar session and choose template li under new session.
4. Go to area definition and highlight region to be measured.
5. Go to toolbar steps and choose measure.
6. Choose 485/527nM filter pair and click measure from steps.
7. Save data from toolbar sheet.
8. Cell viability is proportional to emission detected at 527 nM

Periodic acid Schiff (PAS) staining method

Purpose:

Exam mucin production of HT29/MTX

Principle:

PAS techniques involve two chemical reactions: 1. the oxidation of 1, 2-glycol groups to aldehydes and 2. the reaction of resulting aldehydes with Schiff reagent to produce a purple color.

In this experiment, the periodic acid is used to break the carbon chains of the polysaccharides containing the 1, 2-glycol groups in mucin and to oxidize the broken ends into aldehyde groups. Then Schiff reagent is added to stain resultant aldehydes purple (60).

Materials:

Procedure: tweezers, burner, razor blade, ethanol, PFA (polyformaldehyde), JB-4 plus solution kit (Polysciences, Inc) , benzoyl peroxide, chucks, wax, Schiff's reagent, periodic acid, microtumb (LKB), parafilm, transwell © polycarbonate filters (Corning),

Procedure:

For PAS staining, the co-culture is grown in 12-well polycarbonate transwell and cells was processed at day 3, day 6,day 9, day 12, day 15, day 18 and day 21.

1. Dip a tweezers into 70% ethanol and flame it above a burner under fume hood.
2. Pick one insert with the sterilized tweezers and then place it on the parafilm.

3. Use a razor blade to cut the membrane off from the insert and then excise the membrane from the middle.

4. Fix membranes in 4% PFA for 2 hours at 4 °C.

5. Wash membranes 3 times with PBS.

6. Dehydrate cells through 70, 80, 90 and 100% ethanol (30 minutes for each).

7. Incubate membranes in 5 ml infiltrating reagent (5 ml JB-4 plus solution A+0.0625 gm benzoyl peroxide) overnight to infiltrate cells.

8. Mix 5 ml JB-4 plus solution A with 0.2 ml solution B thoroughly and immediately fill the molds to just above the lower compartment.

9. Stand one membrane in the lower compartment.

10. Place a chuck on the lower compartment, seal the edge of the chuck with wax, and tape over the central hole.

11. Put the mold in fridge overnight.

12. Take the embedded membrane out and stabilize on the microtumb.

13. Cut 1.5 microns thick cell cross-section pieces and spread them in water.

14. Mount the pieces with slides and dry out on a low-power heater.

15. Hydrate cross-section pieces with deionized water for 5 minutes.

16. Incubate slides with 0.5% periodic acid at room temperature for 5 minutes.

17. Rinse in gentle water for 1 minute.

18. Incubate slides in Schiff's reagent for 30 minutes at room temperature.

19. Rinse slides in tap water for 30 min, observe and take photos under 40X objectives.

Alcian blue staining methods

Purpose:

Examine mucin production of HT29/MTX

Principle:

Alcian blue is a group of water-soluble polyvalent basic dyes. The blue color is due to the presence of copper (61, 83). Alcian blue stains both sulfated and carboxylated acid mucopolysaccharides and sulfated and glycoproteins. It is believed that it forms salt linkages with the acid groups of acid mucopolysaccharides. In this study Alcian blue is used to identify acid mucosubstances and acetic mucins

Materials:

Alcian blue (dissolve 0.5 mg Alcian blue in 3% acetic acid), acetic acid, PBS, petri dishes

Procedure:

For Alcian blue staining, the co-culture is grown in petri dishes.

1. Aspirate medium and wash the co-culture with PBS for 3 times.
2. Incubate the co-culture with 4% PFA for 1 hour.
3. Aspirate PFA and rinse with PBS and then 3% acetic acid several times.
4. Stain co-culture with alcian blue for 2 hour.
5. Aspirate alcian blue and rinse with PBS and then 3% acetic acid several times.
6. Observe and take photos under 40X objectives.

Electronic microscopy for co-culture Morphology

Purpose:

Examine morphology of co-culture

Materials:

Ethanol, Karnovkey's solution, tweezers, razor, osmium tetroxide, acetone, epon-araldite (EM Sciences), toluidine blue.

Procedure:

For electronic microscopy, the co-culture is grown in 12-well polycarbonate transwell (Corning) and cells was processed at day 21.

1. Dip a tweezers into 70% ethanol and flame it above a burner under fume hood.

2. Pick one insert with the sterilized tweezers and then place it on the parafilm.

3. Use a razor blade to cut the membrane off from the insert and then excise the membrane from the middle.

4. Fix membranes in Karnovkey's solution for 2 hours at 4 ˚C.

5. Rinse with PBS 3 times.

6. Incubate membranes osmium tetroxide at 4 ˚C for 1 hour.

7. Dehydrate cells through 70, 80, 90 and100% ethanol at -20 ˚C (5 minutes for each).

8. Incubate 50/50 ethanol / acetone for 15 minute and then 100% acetone for15 minute at room temperature.

9. Incubate membranes in the acetone/Epon (50/50) at 4 ˚C overnight and then evaporate acetone overnight.

10. Soak membranes in Epon for seconds and then embed them in molds at 55 °C overnight.

11. Stabilize the embedded membrane on a microtumb and cut 1.5 microns thick pieces with a "boatknife" in which water is filled up to the edge.

12. Remove pieces floating on the water and mount them on slides by heating a low-power heater.

13. Stain cells with toluidine blue, observe and take photos under 40X objectives.

Live/dead assay method

Purpose:

Measure cell viability after treatment

Principle:

Calcein AM is a fluorescent cell marker widely used to measure cell viability. Calcein AM is membrane-permeant and thus can be introduced into cells by incubation. Once inside cells, endogenous esterase hydrolyzes Calcein AM into the highly negatively charged green fluorescent Calcein, which is retained in the cytoplasm. The number of viable cells is proportional to the emission of Calcein trapped in cells (64).

Ethidium bromide (EtBr) is commonly used in molecular biology laboratories as a non-radioactive marker for identifying dead cells. EtBr enters cells with damaged membrane and stains nucleic acid (65). Its emission is intensified 20 times after binding to DNA.

Materials:

Calcein AM, ethidium bromide, PBS, formaldyhyde.

Procedure:

For the Live/dead assay, the co-culture is grown in 96-well black well plates.

1. For each treatment group, two columns are processed. The control group is treated with culture medium and positive control formaldyhyde.
2. Aspirate after incubation for 30 minutes and wash with PBS 3 times.
3. Add 100 uL of 5 um Calcein AM to each well in one row, 100 uL of 2 ug ethidium bromide each well in the other row.
4. Aspirate dye after incubation for 30 minutes and wash with PBS 3 times.

5. Go to toolbar session and choose template li under new session.

6. Go to area definition and highlight region to be measured.

7. Go to toolbar steps and choose measure.

8. Choose 485/527 nM and 527 /544 nM filter pair and click measure from steps.

9. Save data from toolbar sheet.

10. Cell adhesion is proportional to emission detected at 527 nM

11. The number of live cells is proportional to emission detected at 527 nM and the number of dead cells is proportional to emission detected at 590 nM.

Cell adhesion assay method

Purpose:

Measure cell adhesion after treatment

Principle:

Calcein AM is a fluorescent cell marker widely used to measure cell viability. Calcein AM is membrane-permeant and thus can be introduced into cells by incubation. Once inside cells, endogenous esterase hydrolyzes Calcein AM into the highly negatively charged green fluorescent Calcein, which is retained in the cytoplasm. The number of viable cells is proportional to the emission of Calcein trapped in cells (64).

Materials:

Calcein AM, PBS.

Procedure:

For the Live/dead assay, the co-culture is grown in 96 black well

3. Add 100 uL of 5uM Calcein AM to each well after treatment.
4. Aspirate dye after incubation for 30 minutes and wash with PBS 3 times.

3. Go to toolbar session and choose template li under new session.

4. Go to area definition and highlight region to be measured.

5. Go to toolbar steps and choose measure.

6. Choose 485/527nM filter pair and click measure from steps.

7. Save data from toolbar sheet.

8. Cell adhesion is proportional to emission detected at 527 nM

Mucin preparation

Purpose:

Coat cells with mucin to protect them from damage.

Materials:

NaCl, KCl, porcine mucin (Sigma-Aldrich), chelex-100, glass fiber.

Procedure:

1. Dissolve 250 mg mucin in 10 ml pH 7, 140mmol/L NaCl and 5 mmol/L KCl solution.

2. Add 0.5 g chelex-100 and stir until mucin and chelex-100 are well dissolved.

3. Gently filter solution thorugh glass fiber clogged pipets twice.

4. Aliquot and store in -20°C.

Comet assay method

Purpose:

Exam DNA damage after treatment.

Principle:

The comet assay is a rapid and sensitive technique used to analyze and quantify DNA damage. In the comet assay, first cells are lysed in lysis buffer and unwound in alkaline solution (68). Damaged unwound DNA migrates from nucleus by electrophoresis, forming an image like a "comet", whose head consists of intact DNA and tail contains damaged DNA. Therefore, DNA damage is determined by measuring the extent of DNA liberated from the comet head.

Materials:

Comet slides from Trevigen, 1% Low melting point agarose (dissolve 1g low melting point agarose in 100 ml PBS and heat by microwave until boiled. Cool it in 37 °C water bath for at least 30 min before use), 1 X TBE buffer solution (dissolve 108 g Tris base, 55 g boric acid and 9.3 g EDTA in 1 L distilled water to make 10 X TBE buffer and dilute 10 times to get 10 L 1 X TBE buffer), Fresh 4 °C cold lysis buffer solution (dissolve 73.05 NaCl, 14.61 g EDTA, 0.6 g Tris and 5 ml Triton in 500 ml distilled water to get 500 ml lysis buffer solution), Alkaline solution (dissolve 6 g NaOH pellets, 29.2 g EDTA in 500 ml distilled water to get 500 ml alkaline solution), EDTA , Trypsin, PBS (without Ca^{2+} and Mg^{2+}) , hydrogen peroxide

Procedure:

Note: The whole process should be performed under dim light to avoid the damage to DNA

1. Heat low melting point agarose in water bath until boiled and cool it to 37 °C in 37 °C water bath for at least 30 min before use
2. Incubate cells with oxidant for 30 min.
5. Scrape cells and resuspend in 0.5 ml PBS.
6. Embed 100 ul cells in 1 ml 37 °C low melting point agarose.
7. Add 75 ul low melting point agarose on comet slides and chill in a 4 °C fridge for 20 min.
8. Put comet slides in fresh 4 °C cold lysis buffer solutions under dark for 30 min.

9. Gently dab off lysis buffer solution, transfer comet slides to alkaline solution and incubate for 30 min under dark.
10. Gently dab off alkaline solution, transfer comet slides to 1 X TBE buffer solution and incubate for 5 min under dark.
11. Gently dab off 1 X TBE buffer solution, transfer comet slides to fresh 1 X TBE buffer solution and incubate for 5 min under dark again.
12. Transfer comet slides to an electrophoresis chamber and pour 1 X TBE buffer solution until comet slides were barely covered.
13. Run electrophoresis at 20 volts for 10 min
14. Add 100 ul sybr gold each comet slide and observe under the microscope.

Intracellular enzymes extraction

Principle:

Extract intracellular enzymes for further experiment

Materials:

Cold Ripa solution containing cocktail protein inhibitor, rubber policeman,

Procedure:

1. Aspirate old solution and add 0.5 ml cold Ripa solution to each well.

2. Scrap cells off from bottom with rubber policeman and transfer into a centrifuge tube on ice.

3. Vortex strongly to break cell membrane down.

4. Centrifuge at 13,000 RPM for 10 min and collect supernatant for enzymes analysis.

Protein concentrations measurement

Principle:

Proteins reduce Cu^{+2} to Cu^{+1} in alkaline solution. Formed cuprous cation reacts with bicinchoninic acid, producing purple-colored complexes. These complexes exhibit absorbance at 562 nm. Thus, protein concentration can be measured by detecting absorbance at 562 nm.

Material:

BCA Protein Assay Kit (reagent A, B), commercial bovine serum albumin

Procedure:

1. Preparation of protein standards Dilute know concentration of bovine serum albumin (BSA) to concentrations below:

2. Prepare working solution by mixing reagent A with reagent B at a ratio of 50 to 1

vial	Volume of diluent (ul)	Volume and source of BSA (ul)	Final BAS concentration (ug/ml)
A	0	300 of stock	2000
B	325	325 of stock	1000
C	325	325 of vial B	500
D	325	325 of vial C	250
E	325	325 of vial D	125
F	400	100 of vial E	25
G	400	0	0

and then vortex.

3. Pipette 25 ul of each standard or unknown sample into a microplate in duplicate.

4. Add 200 ul of working solution to each well and shake the plate for several seconds.

5. Cover plate and incubate at 37°C for 30 min.

6. Cool plate to room temperature.

7. Measure the absorbance at 562 nm on a plate reader.

Intracellular GPx activity measurement

Principle:

GPx catalyzes the reduction of hydroperoxide, by oxidizing glutathione (GSH) to oxidized glutathione (GSSG). Resultant GSSC can be reduced to GSH utilizing glutathione reductase (GR) and NADPH (76).

$$\text{R-O-O-H} + 2\text{GSH} \xrightarrow{\text{GPx}} \text{R-O-H} + \text{GSSG} + \text{H}_2\text{O}$$

$$\text{GSSG} + \text{NADPH} + \text{H}^+ \xrightarrow{\text{GR}} 2\text{GSH} + \text{NADP}^+$$

In these coupled reactions, the decrease in NADPH is directly proportional to the consumption of GPx. NADPH concentration can be detected by reading absorbance at 340 nm. Therefore, the decrease in absorbance 340 nm reflects inactivation of GPx. In this assay, hydroperoxides are added to GPx and GPx activity is calculated by measuring the decrease in NADPH.

Material:

Cayman glutathione peroxidase assay kit

Procedure:

1. Dilute 2 ml of assay buffer from vial #1 in 18 ml purified water to obtain solution A.

2. Dilute 2 ml of sample buffer from vial #2 in 18 ml purified water to obtain solution B.

3. Aliquot glutathione peroxidase from vial # 3 into 10 ul per vial to avoid repeated freezing and thawing. Prior to use, dilute 10 ul glutathione peroxidase with 490 ul solution B to obtain solution C.

4. Reconstitute co-substrate mixture from vial #4. Add 2 ml purified water into each vial to get solution D. One vial is enough for 40 wells **(Note: Do not freeze the reconstituted reagent)**.

5. For blank, add 120 ul of solution A and 50 ul of solution D to each well. For positive control, add 100 ul of solution A, 50 ul of solution D and 20 ul of solution C each well. For samples, add 100 ul of solution A, 50 ul of solution D and 20 ul of sample to each well. At least a triplicate is needed. To obtain reproducible results, an absorbance decrease between 0.02 and 0.135 / min is expected. When necessary, samples should be diluted or concentrated.

6. Initiate the reaction by adding 20 ul of hydroperoxide from vial # 5 to each well **(Note: finish this step as quickly as possible)**.

7. Shake for a few sec and read absorbance at 340 nm every minute for at least 5 times **(Note: the initial absorbance of samples should be between 0.5 and 1.2)**.

Result calculation

1. Determine the change in absorbance (Δ A 340) per min by: plotting the absorbance as a function of time to obtain the slope of the linear portion of the curve.
2. Determine the rate of Δ A 340/ min. Subtract Δ A 340/ min of blank to obtain the rate of the standards and sample.
3. Calculate GPx activity. NADPH extinction coefficient is 0.00373

GPx activity= (Δ A 340/ min)/ 0.00373* 0.19/0.02* sample dilution (nmol/min/ml)

Phenol red assay

Principle:

Phenol red crosses cell membrane by transcellular pathway at a slow rate when a cell monolayer maturely forms. Damage to cell monolayer leads to loose cell junctions, which allows a large amount of phenol red to pass monolayer paracellularly. Therefore, permeability of monolayer to phenol red reflects the intactness of a cell monolayer.

Materials:

Phenol red, transwell plates, Dulbecco's Modified Eagle's Medium

Procedure:

1. Prepare phenol red standards by dissolving and plot standard curve.
2. Replace the old culture medium in the apical chamber with 0.5 ml of culture

medium supplemented with phenol red; replace the old culture medium in the basolateral chamber with 1.5 ml of normal culture medium.

3. Transfer culture medium from the basolateral chamber to cuvettes after 1 hour incubation and read its absorbance at 450 nm.
4. Calculate concentrations of phenol red in the basolateral chamber based on the standard curve.

Intracellular oxidative status (DHR assay)

Principle:

Dihydrorhodamine 123 (DHR) is a non-fluorescent dye, which readily enters cells and is oxidized to rhodamine 123. Rhodamine 123 localizes in the mitochondria and emits a bright fluorescence upon excitation. Therefore, DHR is a good probe to detect intracellular oxidative stress (67).

Materials:

Dihydrorhodamine 123

Procedure:

For the Live/dead assay, the co-culture is grown in 96 black well

1. Add 100 uL of 20 uM Dihydrorhodamine 123 to each well.
2. Aspirate dye after incubation for 30 minutes and wash with PBS 3 times.
3. Induce different treatments to cells.
4. Aspirate and wash cells with PBS 3 times.
5. Go to toolbar session and choose template li under new session.
6. Go to area definition and highlight region to be measured.

7. Go to toolbar steps and choose measure.

8. Choose 485/527nM filter pair and click measure from steps.

9. Save data from toolbar sheet.

10. Cell adhesion is proportional to emission detected at 527 nM

References

1. Anderson D 2004 Handbook of pediatric nutrition. Jones and Bartlett publishers, Sudbury, Massachusetts.
2. Saugstad OD 2005 Oxygen for newborns: how much is too much? J Perinatol 25 Suppl 2:S45-49; discussion S50.
3. Saugstad OD 1990 Oxygen toxicity in the neonatal period. Acta Paediatr Scand 79:881-892.
4. Cervantes-Munguia R, Espinosa-Lopez L, Gomez-Contreras P, Hernandez-Flores G, Dominguez-Rodriguez J, Bravo-Cuellar A 2006 [Retinopathy of prematurity and oxidative stress]. An Pediatr (Barc) 64:126-131.
5. Moison RM, de Beaufort AJ, Haasnoot AA, Dubbelman TM, van Zoeren-Grobben D, Berger HM 1997 Uric acid and ascorbic acid redox ratios in plasma and tracheal aspirate of preterm babies with acute and chronic lung disease. Free Radic Biol Med 23:226-234.
6. Okur H, Kucukaydin M, Kose K, Kontas O, Dogam P, Kazez A 1995 Hypoxia-induced necrotizing enterocolitis in the immature rat: the role of lipid peroxidation and management by vitamin E. J Pediatr Surg 30:1416-1419.
7. Welty SE 2001 Is there a role for antioxidant therapy in bronchopulmonary dysplasia? J Nutr 131:947S-950S.
8. Friel JK, Martin SM, Langdon M, Herzberg GR, Buettner GR 2002 Milk from mothers of both premature and full-term infants provides better antioxidant protection than does infant formula. Pediatr Res 51:612-618.
9. Shoji H, Oguchi S, Fujinaga S, Shinohara K, Kaneko K, Shimizu T, Yamashiro Y 2005 Effects of human milk and spermine on hydrogen peroxide-induced oxidative damage in IEC-6 cells. J Pediatr Gastroenterol Nutr 41:460-465.
10. Hancock JT, Desikan R, Neill SJ 2001 Role of reactive oxygen species in cell signalling pathways. Biochem Soc Trans 29:345-350.
11. Koppenol WH 2001 The Haber-Weiss cycle--70 years later. Redox Rep 6:229-234.
12. Sies H 1997 Oxidative stress: oxidants and antioxidants. Exp Physiol 82:291-295.
13. Levy MA, Tsai YH, Reaume A, Bray TM 2001 Cellular response of antioxidant metalloproteins in Cu/Zn SOD transgenic mice exposed to hyperoxia. Am J Physiol Lung Cell Mol Physiol 281:L172-182.
14. Adams AK, Wermuth EO, McBride PE 1999 Antioxidant vitamins and the prevention of coronary heart disease. Am Fam Physician 60:895-904.
15. Shoji H, Oguchi S, Shinohara K, Shimizu T, Yamashiro Y 2007 Effects of iron-unsaturated human lactoferrin on hydrogen peroxide-induced oxidative damage in intestinal epithelial cells. Pediatr Res 61:89-92.

16. Liu H, Zheng F, Cao Q, Ren B, Zhu L, Striker G, Vlassara H 2006 Amelioration of oxidant stress by the defensin lysozyme. Am J Physiol Endocrinol Metab 290:E824-832.
17. Hertog MG, Feskens EJ, Hollman PC, Katan MB, Kromhout D 1993 Dietary antioxidant flavonoids and risk of coronary heart disease: the Zutphen Elderly Study. Lancet 342:1007-1011.
18. Brigelius-Flohe R, Kluth D, Banning A 2005 Is there a future for antioxidants in atherogenesis? Mol Nutr Food Res 49:1083-1089.
19. Risk Factors for Preterm Labor and Birth.
20. Joseph KS, Kramer MS, Marcoux S, Ohlsson A, Wen SW, Allen A, Platt R 1998 Determinants of preterm birth rates in Canada from 1981 through 1983 and from 1992 through 1994. N Engl J Med 339:1434-1439.
21. Ward RM, Beachy JC 2003 Neonatal complications following preterm birth. Bjog 110 Suppl 20:8-16.
22. Yeo SL 2006 NICU update: state of the science of NEC. J Perinat Neonatal Nurs 20:46-50.
23. Liu D, Matthews J 2007 Is there an optimal surgical treatment for infants with perforated necrotizing enterocolitis? Nat Clin Pract Gastroenterol Hepatol 4:18-19.
24. Li LQ, Wu B, Gao XX, Wang SX, Zheng ZS, Xu JL 2006 [Role of probiotics in the prevention of neonatal necrotizing enterocolitis: A case-control study]. Zhongguo Dang Dai Er Ke Za Zhi 8:464-466.
25. Gitto E, Reiter RJ, Karbownik M, Xian-Tan D, Barberi I 2001 Respiratory distress syndrome in the newborn: role of oxidative stress. Intensive Care Med 27:1116-1123.
26. Kluckow M 2005 Low systemic blood flow and pathophysiology of the preterm transitional circulation. Early Hum Dev 81:429-437.
27. Biri A, Onan A, Devrim E, Babacan F, Kavutcu M, Durak I 2006 Oxidant status in maternal and cord plasma and placental tissue in gestational diabetes. Placenta 27:327-332.
28. Rickett GM, Kelly FJ 1990 Developmental expression of antioxidant enzymes in guinea pig lung and liver. Development 108:331-336.
29. Dobashi K, Asayama K, Hayashibe H, Munim A, Kawaoi A, Morikawa M, Nakazawa S 1993 Immunohistochemical study of copper-zinc and manganese superoxide dismutases in the lungs of human fetuses and newborn infants: developmental profile and alterations in hyaline membrane disease and bronchopulmonary dysplasia. Virchows Arch A Pathol Anat Histopathol 423:177-184.
30. Inder T, Mocatta T, Darlow B, Spencer C, Volpe JJ, Winterbourn C 2002 Elevated free radical products in the cerebrospinal fluid of VLBW infants with cerebral white matter injury. Pediatr Res 52:213-218.
31. Buonocore G, Perrone S, Longini M, Vezzosi P, Marzocchi B, Paffetti P, Bracci R 2002 Oxidative stress in preterm neonates at birth and on the seventh day of life. Pediatr Res 52:46-49.

32. Saugstad OD 2001 Is oxygen more toxic than currently believed? Pediatrics 108:1203-1205.
33. Callen J, Pinelli J 2005 A review of the literature examining the benefits and challenges, incidence and duration, and barriers to breastfeeding in preterm infants. Adv Neonatal Care 5:72-88; quiz 89-92.
34. Lucas A, Cole TJ 1990 Breast milk and neonatal necrotising enterocolitis. Lancet 336:1519-1523.
35. Anderson JW, Johnstone BM, Remley DT 1999 Breast-feeding and cognitive development: a meta-analysis. Am J Clin Nutr 70:525-535.
36. Aycicek A, Erel O, Kocyigit A, Selek S, Demirkol MR 2006 Breast milk provides better antioxidant power than does formula. Nutrition 22:616-619.
37. Goldman AS, Thorpe LW, Goldblum RM, Hanson LA 1986 Anti-inflammatory properties of human milk. Acta Paediatr Scand 75:689-695.
38. Shoji H, Oguchi S, Shimizu T, Yamashiro Y 2003 Effect of human breast milk on urinary 8-hydroxy-2'-deoxyguanosine excretion in infants. Pediatr Res 53:850-852.
39. Dewey KG 2001 Nutrition, growth, and complementary feeding of the breastfed infant. Pediatr Clin North Am 48:87-104.
40. Miller JL, Kang SM 2007 Preliminary ultrasound observation of lingual movement patterns during nutritive versus non-nutritive sucking in a premature infant. Dysphagia 22:150-160.
41. Lau C, Smith EO, Schanler RJ 2003 Coordination of suck-swallow and swallow respiration in preterm infants. Acta Paediatr 92:721-727.
42. Singer LT, Salvator A, Guo S, Collin M, Lilien L, Baley J 1999 Maternal psychological distress and parenting stress after the birth of a very low-birth-weight infant. Jama 281:799-805.
43. McGuire W, Henderson G, Fowlie PW 2004 Feeding the preterm infant. Bmj 329:1227-1230.
44. Boyd CA, Quigley MA, Brocklehurst P 2007 Donor breast milk versus infant formula for preterm infants: systematic review and meta-analysis. Arch Dis Child Fetal Neonatal Ed 92:F169-175.
45. Bode S, Dreyer M, Greisen G 2004 Gastric emptying and small intestinal transit time in preterm infants: a scintigraphic method. J Pediatr Gastroenterol Nutr 39:378-382.
46. Omari TI, Davidson GP 2003 Multipoint measurement of intragastric pH in healthy preterm infants. Arch Dis Child Fetal Neonatal Ed 88:F517-520.
47. Armand M, Hamosh M, Mehta NR, Angelus PA, Philpott JR, Henderson TR, Dwyer NK, Lairon D, Hamosh P 1996 Effect of human milk or formula on gastric function and fat digestion in the premature infant. Pediatr Res 40:429-437.
48. Etcheverry P, Wallingford JC, Miller DD, Glahn RP 2004 Calcium, zinc, and iron bioavailabilities from a commercial human milk fortifier: a comparison study. J Dairy Sci 87:3629-3637.

49. Buller HA, Rings EH, Montgomery RK, Grand RJ 1991 Clinical aspects of lactose intolerance in children and adults. Scand J Gastroenterol Suppl 188:73-80.
50. Chantret I, Rodolosse A, Barbat A, Dussaulx E, Brot-Laroche E, Zweibaum A, Rousset M 1994 Differential expression of sucrase-isomaltase in clones isolated from early and late passages of the cell line Caco-2: evidence for glucose-dependent negative regulation. J Cell Sci 107 (Pt 1):213-225.
51. Galvan EM, Roth GA, Monferran CG 2006 Functional interaction of Escherichia coli heat-labile enterotoxin with blood group A-active glycoconjugates from differentiated HT29 cells. Febs J 273:3444-3453.
52. Shulman RJ, Wong WW, Smith EO 2005 Influence of changes in lactase activity and small-intestinal mucosal growth on lactose digestion and absorption in preterm infants. Am J Clin Nutr 81:472-479.
53. Sambuy Y, De Angelis I, Ranaldi G, Scarino ML, Stammati A, Zucco F 2005 The Caco-2 cell line as a model of the intestinal barrier: influence of cell and culture-related factors on Caco-2 cell functional characteristics. Cell Biol Toxicol 21:1-26.
54. Hilgendorf C, Spahn-Langguth H, Regardh CG, Lipka E, Amidon GL, Langguth P 2000 Caco-2 versus Caco-2/HT29-MTX co-cultured cell lines: permeabilities via diffusion, inside- and outside-directed carrier-mediated transport. J Pharm Sci 89:63-75.
55. Pontier C, Pachot J, Botham R, Lenfant B, Arnaud P 2001 HT29-MTX and Caco-2/TC7 monolayers as predictive models for human intestinal absorption: role of the mucus layer. J Pharm Sci 90:1608-1619.
56. Huet C, Sahuquillo-Merino C, Coudrier E, Louvard D 1987 Absorptive and mucus-secreting subclones isolated from a multipotent intestinal cell line (HT-29) provide new models for cell polarity and terminal differentiation. J Cell Biol 105:345-357.
57. de Nonancourt-Didion M, Gueant JL, Adjalla C, Chery C, Hatier R, Namour F 2001 Overexpression of folate binding protein alpha is one of the mechanism explaining the adaptation of HT29 cells to high concentration of methotrexate. Cancer Lett 171:139-145.
58. Lesuffleur T, Barbat A, Dussaulx E, Zweibaum A 1990 Growth adaptation to methotrexate of HT-29 human colon carcinoma cells is associated with their ability to differentiate into columnar absorptive and mucus-secreting cells. Cancer Res 50:6334-6343.
59. Frisk T, Rydholm S, Andersson H, Stemme G, Brismar H 2005 A concept for miniaturized 3-D cell culture using an extracellular matrix gel. Electrophoresis 26:4751-4758.
60. Humason. GL 1967 Animal Tissure Techniques. W.H Freeman and Company, San Francisco.
61. Sheehan DH, B 1980 Theory and practice of HIstotechnology. Battelle Press, Ohio.

62. Mukherjee T, Squillantea E, Gillespieb M, Shao J 2004 Transepithelial electrical resistance is not a reliable measurement of the Caco-2 monolayer integrity in Transwell. Drug Deliv 11:11-18.
63. Neri S, Mariani E, Meneghetti A, Cattini L, Facchini A 2001 Calcein-acetyoxymethyl cytotoxicity assay: standardization of a method allowing additional analyses on recovered effector cells and supernatants. Clin Diagn Lab Immunol 8:1131-1135.
64. Chaka W, Scharringa J, Verheul AF, Verhoef J, Van Strijp AG, Hoepelman IM 1995 Quantitative analysis of phagocytosis and killing of Cryptococcus neoformans by human peripheral blood mononuclear cells by flow cytometry. Clin Diagn Lab Immunol 2:753-759.
65. Gray DW, Morris PJ 1987 The use of fluorescein diacetate and ethidium bromide as a viability stain for isolated islets of Langerhans. Stain Technol 62:373-381.
66. Shanker G, Aschner JL, Syversen T, Aschner M 2004 Free radical formation in cerebral cortical astrocytes in culture induced by methylmercury. Brain Res Mol Brain Res 128:48-57.
67. Yi J, Gao F, Shi G, Li H, Shi X, Tang X 2002 Apoptosis susceptibility of tumor cells to arsenic trioxide and the inherent cellular level of reactive oxygen species. Chin Med J (Engl) 115:603-606.
68. Tice RR, Agurell E, Anderson D, Burlinson B, Hartmann A, Kobayashi H, Miyamae Y, Rojas E, Ryu JC, Sasaki YF 2000 Single cell gel/comet assay: guidelines for in vitro and in vivo genetic toxicology testing. Environ Mol Mutagen 35:206-221.
69. de Lima Leite A, Ferreira Santiago Junior J, Mauad Levy F, Gutierrez Maria A, da Silva Fernandes M, Favero Salvadori DM, Araki Ribeiro D, Afonso Rabelo Buzalaf M 2007 Absence of DNA damage in multiple organs (blood, liver, kidney, thyroid gland and urinary bladder) after acute fluoride exposure in rats. Hum Exp Toxicol 26:435-440.
70. Jin F, Welch R, Glahn R 2006 Moving toward a more physiological model: application of mucin to refine the in vitro digestion/Caco-2 cell culture system. J Agric Food Chem 54:8962-8967.
71. Friel JK, Diehl-Jones WL, Suh M, Tsopmo A, Shirwadkar VP 2007 Impact of iron and vitamin C-containing supplements on preterm human milk: in vitro. Free Radic Biol Med 42:1591-1598.
72. Jovani M, Barbera R, Farre R, Martin de Aguilera E 2001 Calcium, iron, and zinc uptake from digests of infant formulas by Caco-2 cells. J Agric Food Chem 49:3480-3485.
73. Walter E, Janich S, Roessler BJ, Hilfinger JM, Amidon GL 1996 HT29-MTX/Caco-2 cocultures as an in vitro model for the intestinal epithelium: in vitro-in vivo correlation with permeability data from rats and humans. J Pharm Sci 85:1070-1076.

74. Yun S, Habicht JP, Miller DD, Glahn RP 2004 An in vitro digestion/Caco-2 cell culture system accurately predicts the effects of ascorbic acid and polyphenolic compounds on iron bioavailability in humans. J Nutr 134:2717-2721.
75. Biziukin AV, Korkina LG, Velichkovskii BT 1995 [Comparative use of 2,7-dichlorofluorescein diacetate, dihydrorhodamine 123, and hydroethidine for studying oxidative metabolism of phagocytosing cells]. Biull Eksp Biol Med 119:361-365.
76. Udler M, Maia AT, Cebrian A, Brown C, Greenberg D, Shah M, Caldas C, Dunning A, Easton D, Ponder B, Pharoah P 2007 Common germline genetic variation in antioxidant defense genes and survival after diagnosis of breast cancer. J Clin Oncol 25:3015-3023.
77. Wu LL, Chiou CC, Chang PY, Wu JT 2004 Urinary 8-OHdG: a marker of oxidative stress to DNA and a risk factor for cancer, atherosclerosis and diabetics. Clin Chim Acta 339:1-9.
78. De Boeck M, Touil N, De Visscher G, Vande PA, Kirsch-Volders M 2000 Validation and implementation of an internal standard in comet assay analysis. Mutat Res 469:181-197.
79. Glahn RP, Lai C, Hsu J, Thompson JF, Guo M, Van Campen DR 1998 Decreased citrate improves iron availability from infant formula: application of an in vitro digestion/Caco-2 cell culture model. J Nutr 128:257-264.
80. Ait-Oukhatar N, Bouhallab S, Bureau F, Arhan P, Maubois JL, Bougle DL 2000 In vitro digestion of caseinophosphopeptide-iron complex. J Dairy Res 67:125-129.
81. Bosscher D, Lu Z, Janssens G, Van Caillie-Bertrand M, Robberecht H, De Rycke H, De Wilde R, Deelstra H 2001 In vitro availability of zinc from infant foods with increasing phytic acid contents. Br J Nutr 86:241-247.
82. Fuller E, Duckham C, Wood E 2007 Disruption of epithelial tight junctions by yeast enhances the paracellular delivery of a model protein. Pharm Res 24:37-47.
83. Bancroft JS, A 1982 Theory and Practice of Histological Techniques. Churchill Livingstone, New York.